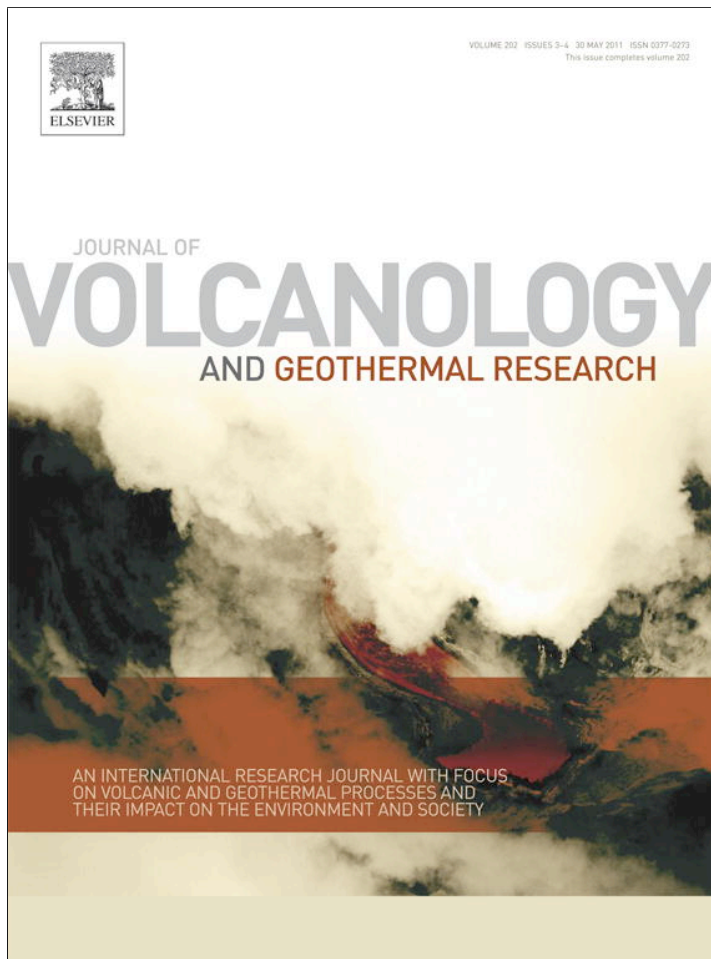


Provided for non-commercial research and education use.
Not for reproduction, distribution or commercial use.



This article appeared in a journal published by Elsevier. The attached copy is furnished to the author for internal non-commercial research and education use, including for instruction at the authors institution and sharing with colleagues.

Other uses, including reproduction and distribution, or selling or licensing copies, or posting to personal, institutional or third party websites are prohibited.

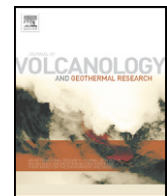
In most cases authors are permitted to post their version of the article (e.g. in Word or Tex form) to their personal website or institutional repository. Authors requiring further information regarding Elsevier's archiving and manuscript policies are encouraged to visit:

<http://www.elsevier.com/copyright>



Contents lists available at ScienceDirect

Journal of Volcanology and Geothermal Research

journal homepage: www.elsevier.com/locate/jvolgeores

Evidence for Late Pleistocene uplift at the Somma-Vesuvius apron near Pompeii

Aldo Marturano ^{a,*}, Giuseppe Aiello ^b, Diana Barra ^b^a Istituto Nazionale di Geofisica e Vulcanologia, sez. Osservatorio Vesuviano, via Diocleziano 328, 80124 Naples, Italy^b Dipartimento di Scienze della Terra, Università di Napoli Federico II, 80136 Naples, Italy

ARTICLE INFO

Article history:

Received 28 October 2010

Accepted 21 February 2011

Available online 4 March 2011

Keywords:

ground uplift

Somma-Vesuvius

Pleistocene

Palaeoecology

benthic foraminifers

ostracods

ABSTRACT

Detailed stratigraphic and micropalaeontological analyses of samples from boreholes at the Somma-Vesuvius apron, between Pompeii and the sea, allowed reconstruction of Late Quaternary palaeoenvironmental evolution of the Sarno coastal plain. In all, 116 samples were recovered from seven boreholes drilled from 2–10 m a.s.l. to 16.5–26 m b.s.l. Microfossil assemblages, with special regard to benthic foraminifers and ostracods, were used to reconstruct the depositional palaeoenvironment. Fossil remains show that all the pre-79 AD fossiliferous sediments from 2 to –24 m a.s.l. were deposited in shallow marine waters for a long time despite an appreciable sea level rise. The data indicate alternation of both shallow marine and subaerial conditions during the last ~15 kyr, evidencing ground uplift of the area of about 75 m at a rate of ~5 mm/year. Marine sediment accumulation (~6 m/kyr) and tectonic uplift long offset the sea level rise, and as a consequence, submerged areas remained the same as well.

© 2011 Elsevier B.V. All rights reserved.

1. Introduction

The south-eastern side of the Somma-Vesuvius volcano is a densely inhabited area including the towns of Boscorecase, Boscoreale, Torre Annunziata, Scafati, the archaeological site of Pompeii and present-day town of Pompei (Fig. 1). The Somma-Vesuvius volcano formed mostly during the last 25 ka, producing at least three Plinian eruptions before AD 79 ($22\ 030 \pm 175$ cal BP "Pomice di Base", 8890 ± 90 cal BP "Mercato", and 4365 ± 40 cal BP "Avellino") and many smaller-scale subplinian eruptions (Santacroce and Sbrana, 2003; Santacroce et al., 2008 and references therein).

The world famous Roman city of Pompeii and other sites were buried by the AD 79 Vesuvius eruption. The sketch in Fig. 1 shows the apron of the volcano where the transition between the volcano flanks and the alluvial plain occurs. It represents the south-western stretch of the Sarno Plain, a Late Quaternary alluvial coastal plain where the River Sarno flows. The Sarno Plain is located in the southern part of the Campanian Plain, a Quaternary basin bordered by faults that affected the Mesozoic and Cenozoic calcareous rocks of the Apennine thrust belt. It is a NE–SW elongated structural depression bordered on the N-E and S-E by Mesozoic carbonate rocks, on the S-W by the Tyrrhenian Sea and on the N-W by Somma-Vesuvius. The geological evolution of the Sarno Plain has been the subject of numerous publications including stratigraphic, rock dating and micropalaeontological studies (Barra et al., 1989; Patacca et al.,

1990; Albore Livadie et al., 1991; Brancaccio et al., 1991; Cinque, 1991; Barra, 1992; Barra et al., 1992a; Cinque et al., 1993; Brocchini et al., 2001; Cinque and Irollo, 2004; Sacchi et al., 2005; Acocella and Funiciello, 2006; Vogel and Märker, 2010).

The Somma-Vesuvius complex and the Sarno Plain are generally thought to have experienced a period of subsidence, within the global tectonic subsidence context of the Campanian Plain with respect to the bordering carbonates (e.g. Cinque and Russo, 1986; Albore Livadie et al., 1991; Brocchini et al., 2001; Ferranti et al., 2006; Di Renzo et al., 2007). During the Holocene transgression maximum, the sea reached an area more than 3 km inland of the present shoreline, cutting into the volcano at its foot near ancient Pompeii (Cinque and Russo, 1986; Albore Livadie et al., 1991; Barra, 1992; Pescatore et al., 1999, 2001). Recently, Marturano et al. (2009) detected ~30 m uplift at Pompeii which occurred at a rate of ~5 mm/year in the Holocene. Although the uplift was assumed extended to the whole Somma-Vesuvius structure, a very local cause was not excluded.

The objective of this study was to ascertain whether the Vesuvian apron close to Pompeii experienced ground movements such as those at the famous archaeological site, conditioning post-glacial sea ingressions. A chance to obtain direct information on the subsurface geology of the area was provided by cores and drilling logs carried out for projects and geotechnical surveys. The study area (Fig. 2) extends on land from the archaeological site of Pompeii to the sea. Here we present new micropalaeontological analyses of samples drilled during the CNR project "Progetto Finalizzato Beni Culturali, Sottoprogetto 4". In order to evidence Late Quaternary interglacial transgression areas and possible uplift events, Cultural Heritage (BC) data were integrated with those recently reported for the archaeological site of Pompeii (CA in

* Corresponding author.

E-mail address: marturano@ov.ingv.it (A. Marturano).

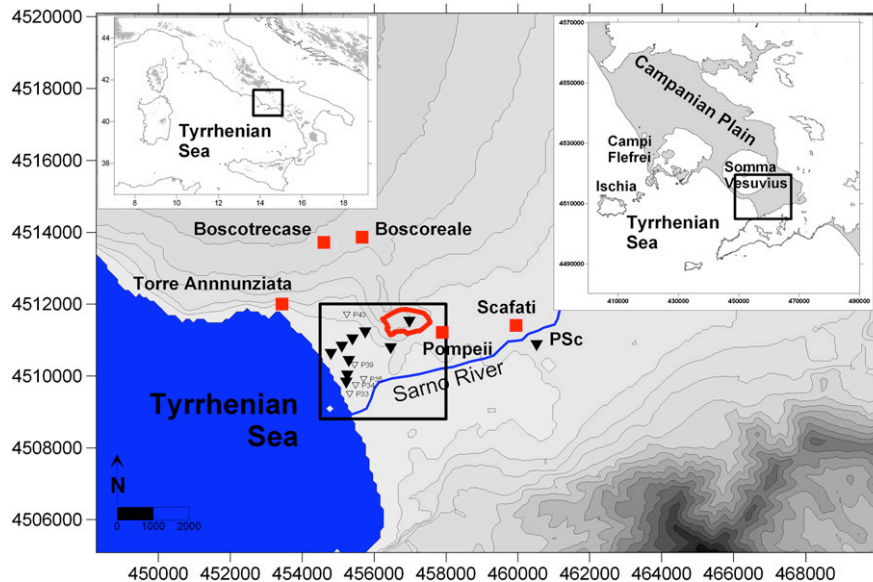


Fig. 1. Vesuvius and study area (framed). Boreholes (triangles) and localities (squares). PSc borehole is located eastward of the study area near the Sarno River.

Fig. 2) by Marturano et al. (2009) and the A14 core (A14 in Fig. 2) by Di Vito et al. (1998). By integrating all the data: a) it was verified that the sites experienced both subaerial and marine conditions from the Last Glacial Maximum; b) the shoreline of the maximum ingression was shifted well beyond the scarp on the southern side of ancient Pompeii; c) a longer-term uplift trend was observed to affect the study area consistent with the site of Pompeii. Below we aim to reconstruct the depositional palaeoenvironment of the study area. Its tectonic evolution will then be proposed.

2. Palaeoecology

2.1. Materials and methods

Samples were recovered from seven boreholes drilled outside the ancient site of Pompeii situated along two transects (Transect 1: BC 1–4; Transect 2: BC 5–7) at 2–10 m a.s.l. Borehole depths ranged from 16.5 to 26 m (Fig. 3). Calcareous remains include benthic foraminifer tests, ostracod shells, bryozoan and mollusc (bivalve, gastropod and,

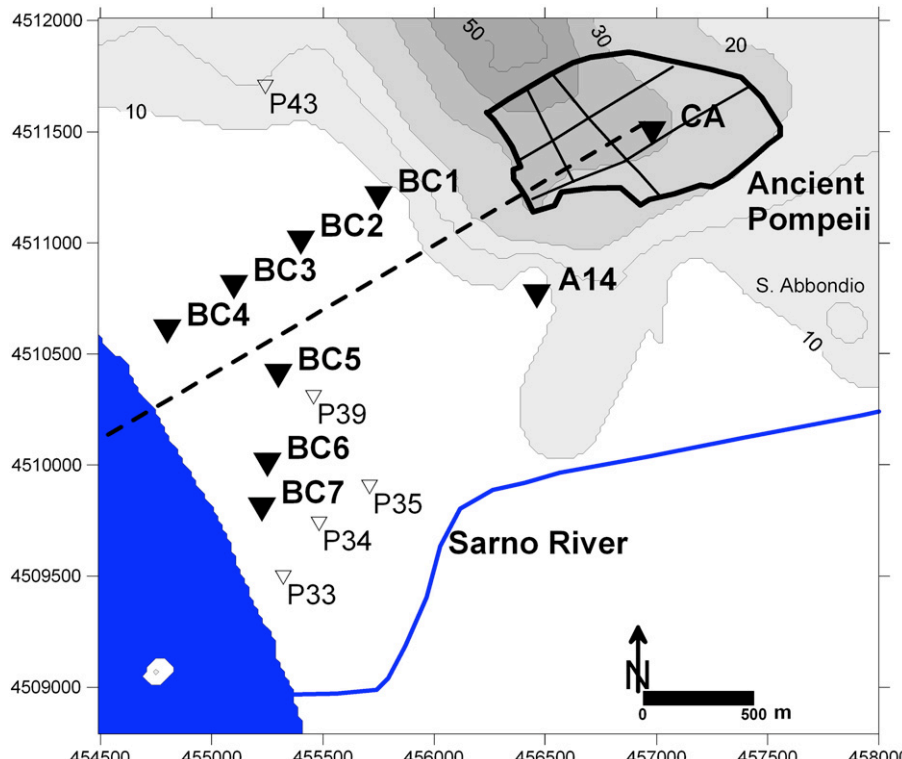


Fig. 2. Study area. Location of boreholes (triangles): (BC1–7) Beni Culturali Project; (CA) Insula of Casti Amanti within Ancient Pompeii; (A14) A14 core; (P33, 34, 35, 39, 43) previous boreholes (Barra, 1992). The same symbols, the coast and the course of the Sarno River are used as landmarks in the next figures.

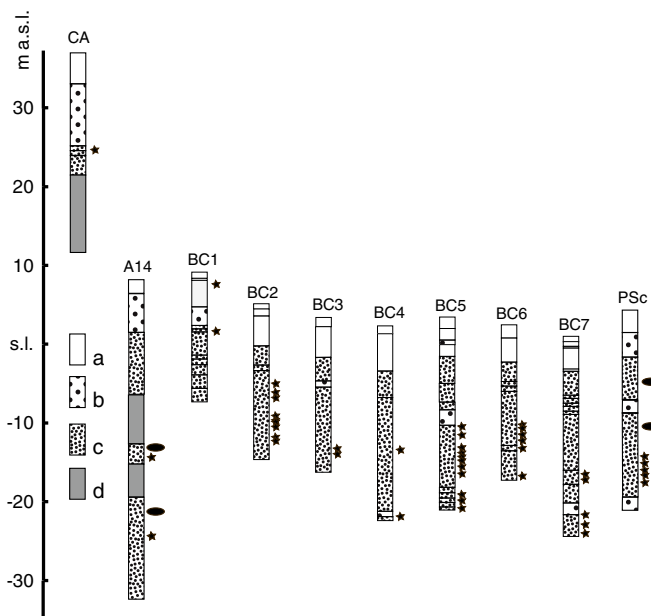


Fig. 3. Schematic stratigraphic columns of boreholes (for location see Figs. 1, and 2). a) Post 79 AD sediments; b) pumice deposits; c) sands, clays, palaeosols and humified layers; d) block lavas and scoria. Stars represent marine fossiliferous samples (see Table 1); ellipses the ^{14}C dated samples.

infrequently, scaphopod) fragments, echinoid spines and very rare brachiopods.

Assemblages of benthic foraminifers and ostracods were used to reconstruct the depositional palaeoenvironment of Quaternary sediments in the Sarno coastal plain. A total of 116 samples (Table 1) were examined. Each core sample was cleaned to remove surface material in contact with drilling mud. Samples were disaggregated using hydrogen peroxide and washed through a 63- μm mesh; the dried samples were sieved to obtain the >125- μm fraction. Benthic foraminifers and ostracods, picked out from the coarser fraction, were recorded in 37 samples. Three samples, devoid of foraminifers and ostracods, yielded bryozoan or bivalve remains, and 76 were barren. All species are given a semi-quantitative rating, according to their relative abundance: rare (1–3 specimens), uncommon (4–7 specimens), common (8–20 specimens), abundant (> 20 specimens).

In all, 61 benthic foraminifer species, pertaining to 27 genera, and 53 species from 26 genera of ostracods were identified and listed (Table 2; Appendix A). Eight species are left in open nomenclature and four given affinitive status: *Aurila* sp., *Callistocythere* sp., *Neonesidea* sp., *Propontocypris* sp. because only young instars were found; *Hemicytherura* sp., *Pseudocytherura* aff. *P. strangulata*, *Sahnicythere* sp., *Sclerochilus* sp., *Semicytherura* aff. *S. diafora*, *S. aff. S. paradoxa*, *Xestoleberis* aff. *X. labiata*, *Xestoleberis* sp. due to the poor preservation of the material. One erased valve of a freshwater candonid species was considered allochthonous (i.e. transported from continental waters).

2.2. Palaeoenvironmental interpretation

All of the autochthonous species found in the study area are marine and presently living in the Mediterranean. Areal and bathymetric distribution, as well as the assemblages characteristic of different biotopes, are well defined in the literature. Data on benthic foraminifers are taken from Le Calvez and Le Calvez (1958), Blanc-Vernet (1969), Pujos (1976), Haake (1977), Blanc-Vernet et al. (1979), Vénec-Peyré (1984), Sgarrella and Barra (1985), Jorissen (1987),

Sgarrella et al. (1985), Sgarrella and Moncharmont Zei (1993), Donnici and Serandrei Barbero (2002), Aiello et al. (2006) and Frezza and Carboni (2009); ostracod data are reported by Müller (1894), Rome (1964), Barbeito-Gonzalez (1971), Uffenorde (1972), Breman (1976), Bonaduce et al. (1976, 1977, 1988), Yassini (1979), Peyrouquet and Nachite (1984), Arbulia et al. (2001, 2004), Triantaphyllou et al. (2005) and Aiello et al. (2006). Information from ecological literature was integrated with unpublished data on Recent Mediterranean assemblages (Aiello and Barra).

On the basis of the known distributional data (depth range, sedimentary substrate, and presence of marine vegetation) five groups of species were defined:

- (1) Species found exclusively or preferentially in the infralittoral zone, on sand, silt and muddy sand, without vegetation.
Benthic foraminifers: *Adelosina elegans*, *A. longirostra*, *Ammonia tepida*, *A. parkinsoniana*, *A. perlucida*, *Astrononion stelligerum*, *Elphidium complanatum*, *E. crispum*, *E. cuvillieri*, *E. incertum*, *E. punctatum*, *Elphidium* sp. A, *Quinqueloculina bosciana*, *Q. poeyana*, *Q. lamarciana*, *Q. stelligera*, *Sigmoilina tricosta*, *Triloculina gibba*, *T. schreibersiana*.
Ostracods: *Aurila prasina*, *Callistocythere protracta*, *Cytheretta adriatica*, *C. subradiosa*, *Eucytherura angulata*, *Hemicytherura gracilicosta*, *Heterocythereis voraginosa*, *Leptocythere bituberculata*, *L. macella*, *L. ramosa*, *Loxoconcha affinis*, *L. ovulata*, *Pontocythere turbida*, *Semicytherura incongruens*, *S. sulcata*, *Urocythereis flexicauda*, *U. margaritifera*.
- (2) Species found exclusively or preferentially in the infralittoral zone with vegetation cover.
Benthic foraminifers: *Asterigerinata mamilla*, *Lamarcina scabra*, *Massilina secans*, *Planorbolina mediterranensis*, *Rosalina bradyi*, *R. floridana*, *R. obtusa*, *Sigmoilina grata*, *Triloculina oblunga*, *T. rotunda*.
Ostracods: *Neocytherideis subulata*, *Paradoxostoma triste*, *P. versicolor*, *Pontocypris pellucida*, *Sclerochilus levius*, *Sclerochilus* sp.
- (3) Infralittoral ubiquitous species, associated with sandy to sandy-muddy bottom with vegetated substrate.
Benthic foraminifers: *Buccella granulata*, *Cibicides lobatulus*, *Quinqueloculina berthelotiana*, *Q. lata*, *Siphonaperta aspera*, *Spirillina vivipara*, *Tretomphalus concinnus*, *Triloculina plicata*, *T. trigonula*.
Ostracods: *Leptocythere levis*, *Paldoconcha turbida*, *Semicytherura acuticostata*, *S. paradoxa*, *Tenedocythere prava*, *Xestoleberis communis*, *X. dispar*.
- (4) Species living in the infralittoral to upper circalittoral zones.
Benthic foraminifers: *Adelosina mediterranensis*, *Ammonia gaimardi*, *Bolivina striatula*, *Bulimina elongata*, *Elphidium granosum*, *E. macellum*, *E. pulvereum*, *Lagena clavata*, *Nonionella turgida*, *Quinqueloculina contorta*, *Q. pygmaea*, *Q. seminulum*, *Q. tenuicollis*, *Reussella spinulosa*, *Sigmoilina costata*, *Spirolocolina excavata*, *Stainforthia complanata*, *Textularia calva*.
Ostracods: *Carinocythereis whitei*, *Cistacythereis (H.) turbida*, *Costabatei*, *C. edwardsi*, *Hemicytherura defiorei*, *Microcytherura fulva*, *Semicytherura dispar*, *S. mediterranea*, *S. rarecostata*, *S. stilifera*.
- (5) Species occasionally present in the infralittoral zone, more frequently found on circalittoral muddy substrate.
Benthic foraminifers: *Bulimina aculeata*, *Cornuspira involvens*, *Miliolinella subrotunda*, *Quinqueloculina stalkeri*.
Ostracods: *Eucytherura complexa*.

The fossil assemblages in question are mainly associated to changes in sediment granulometry. Species composition and semi-quantitative assemblage analysis allow different palaeoenvironments to be recognized in the borehole sediments.

Assemblages:

(1) Bryozoan or bivalve fragments, in coarse to medium sands; samples: BC1–51, BC1–45; BC6–133. Upper infralittoral or mesolittoral zone, strongly influenced by high-energy waters.

Table 1

Elevation and dry weight of studied samples; fossiliferous samples are asterisked.

Sample	QC	QA	Weight
<i>Transect 1</i>			
CORE BC 1			
43	0.96	9:04	71
44	1.56	8:44	35
45*	1.82	8.18	42
47	2.40	7.60	41
48	3.20	6.80	27
49	4.00	6.00	41
50	4.37	5.63	35
51*	7.02	2.98	32
52	7.30	2.70	45
54	7.70	2.30	52
59	10.44	−0.44	74
62	12.70	−2.70	40
CORE BC 2			
71	5.80	0.20	52
75*	10.40	−4.40	43
76*	11:23	−5.23	44
78*	12:18	−6.18	56
80	13.38	−7.38	59
81*	14:59	−8.59	36
82*	14.77	−8.77	51
83*	15.50	−9.50	32
84*	15.98	−9.98	57
85*	16.60	−10.60	35
86*	17:55	−11.55	38
87*	18.20	−12.20	49
CORE BC 3			
95	4.50	−0.50	35
100	8.50	−4.5	65
103	10.60	−6.60	58
104	11.55	−7.55	48
105	12.20	−8.20	35
106	13.20	−9.20	44
107	14.77	−10.77	51
108*	17.00	−13.00	38
109*	17.76	−13.76	34
110	18.55	−14.55	42
112	20.16	−16.16	31
CORE BC 4			
178	3.00	0.00	142
179	3.88	−0.88	81
190	10.28	−7.28	63
191	11.12	−8.12	96
192	11.81	−8.81	60
193	12.18	−9.18	45
194	12.48	−9.48	58
195	13.13	−10.13	87
196	14.07	−11.07	62
197	14.85	−11.85	66
198*	15:56	−12.56	67
199	16.11	−13.11	82
200	16.73	−13.73	57
201	17.60	−14.60	46
202	18.02	−15.02	64
203	19.00	−16.00	81
204	19.54	−16.54	82
205	20.50	−17.50	43
206	21.10	−18.10	54
207	21.81	−18.81	56
208	22.64	−19.64	49
209	23.58	−20.58	60
210	24.65	−21.65	65
214*	24.72	−21.72	72
<i>Transect 2</i>			
CORE 5			
152	8.90	−4.90	47
153	10.00	−6.00	28
154	11.60	−7.60	62
156*	14:17	−10.17	56
157*	15.30	−11.30	74
158	16.14	−12.14	26
159*	16.89	−12.89	54
160*	17:39	−13.39	65

Table 1 (continued)

Sample	QC	QA	Weight
<i>Transect 2</i>			
CORE 5			
161*	17.94	−13.94	60
162*	18.50	−14.50	64
163*	19:07	−15.07	65
164*	19:58	−15.58	52
165	20.22	−16.22	20
166	20.94	−16.94	21
167	21.68	−17.68	42
168	22.18	−18.18	28
169*	22.66	−18.66	59
170*	23.27	−19.27	45
171*	23.80	−19.80	41
172*	24.46	−20.46	26
173	24.71	−20.17	50
CORE BC 6			
113	2.30	0.70	46
121	9.15	−6.15	64
122	10.00	−7.00	71
123	11.55	−8.55	105
125*	12.62	−9.62	48
126*	13.20	−10.20	43
127*	14.00	−11.00	31
128*	14.80	−11.80	42
129*	15.75	−12.75	34
130	16.50	−13.50	54
131	17.80	−14.80	35
132	18.35	−15.35	37
CORE BC 7			
1	1.34	0.66	23
2	1.39	0.61	31
5	4.25	−2.25	49
7	6.60	−4.60	66
10	8.10	−6.10	41
11	8.90	−6.90	75
12	9.70	−7.70	54
16	10.90	−8.90	39
17	11.56	−9.56	58
22	14.25	−12.25	47
24	15.50	−13.50	35
28	16.70	−14.70	48
29	17.30	−15.30	40
31*	18.00	−16.00	45
32*	18.60	−16.60	27
34	19.65	−17.65	56
35	20.20	−18.20	48
36	21.5	−19.50	38
37*	23.20	−21.20	33
39*	24.40	−22.40	41
40*	25.00	−23.00	37
42*	26.00	−24.00	38

(2) Rare foraminifers, typical of very shallow waters (*Ammonia parkinsoniana*, *Buccella granulata*, *Elphidium crispum*), very rare echinoid and mollusc remains, in coarse to fine sands; samples: BC2-85, BC2-83, BC2-82, BC2-81, BC2-78, BC2-76; BC4-214; BC5-164, BC5-162, BC5-159; BC6-127, BC6-125. Deposition occurred in high-energy marine waters, within the upper part of the infralittoral zone.

(3) Low abundance and diversity recorded in assemblages A and B and the presence of shell debris indicate a depositional environment ranging from upper infralittoral zone to infralittoral fringe (possibly reaching the mesolittoral zone).

(4) Very rare ostracods, typical of very shallow waters (*Palmostoma turbida*, *Pontocythere turbida*); samples: BC2-75; BC4-198. In the former sample echinoid spines also occur. Medium-fine sands. Upper part of the infralittoral zone.

(5) Relatively rich and well-diversified foraminifer and ostracod assemblages; samples: BC2-87, BC2-86, BC2-84; BC3-109, BC3-108; BC5-

172, BC5-171, BC5-170, BC5-169, BC5-163, BC5-161, BC5-160, BC5-157, BC5-156; BC6-129, BC6-128, BC6-126; BC7-42, BC7-32, BC7-31. Coarse-fine sands to muddy silts. Sedimented within the upper infralittoral zone. A palaeoenvironment frequently characterized by vegetation is inferred from the common presence of phytophilous species.

(6) Rich and diversified assemblages consisting of foraminifer, ostracod, bryozoan, echinoid and mollusc remains. Both foraminifers and ostracod assemblages include very shallow (i.e. upper infralittoral) and lower infralittoral species; samples: BC7-40, BC7-39, BC7-37. The samples are characterized by very fine sands. Assemblages represent the maximum palaeodepth, within the infralittoral zone, probably not exceeding 20 m b.s.l.

Fossil remains show that all the fossiliferous sediments were deposited in shallow marine waters. The palaeoenvironment ranges from the lower infralittoral zone characterized by muddy bottoms with vegetation, low energy and high abundance and diversity of the assemblages, to the upper infralittoral zone, infralittoral fringe and possibly mesolittoral zone with generally coarser sediments, higher energy, lean assemblages and low specific diversity.

The presence in sample BC7-39 of one valve of a freshwater candonid species, clearly transported by fluvial waters, shows the proximity of the Sarno river mouth. The influence of fluvial supply is suggested by the record of a group of foraminiferal species (*A. parkinsoniana*, *A. longirostra*, *Q. seminulum*, *E. granosum*, *T. schreibersiana*, *T. trigonula*), previously reported as common on sandy or pelitic-sandy bottoms in marine environments under the influence of fluvial waters (Pujoz, 1976; Sgarrella and Barra, 1985; Sgarrella et al., 1985; Jorissen, 1988).

Fossiliferous samples pertain to pre-79 AD sequences, while sediments younger than 79 AD are barren except sample BC1-45 which yielded bivalve fragments. Core depth of fossiliferous deposits is generally deeper than 10–15 m b.s.l., except for BC2 that shallows at ~5 m b.s.l.

3. Long-term deformation

Recently Marturano (2008) and Marturano et al. (2009) proposed to extend both single eruption upwelling and long-term ground deformation at the Somma-Vesuvius volcano by utilizing stratigraphic, archaeological, micropalaeontological, archaeometric and petrochemical data from Pompeii. A local cause was not excluded; therefore, new evidence is required to corroborate the hypothesis and it is necessary to take account of volcano-tectonic deformation in stratigraphic, sedimentological and palaeontological analyses performed near the volcano in order to reconstruct the depositional palaeoenvironment.

The Cultural Heritage Project mainly focused on environmental study close to Pompeii and, timewise, close to the 79 AD eruption, thus giving a partial, though detailed, picture of the site evolution (Pescatore et al., 1999, 2001; Ciarallo et al., 2003). Data from the seven project boreholes offer an opportunity to verify the dynamics of the area and, as we are interested in the long-term changes of the apron environment, the sediments older than 79 AD will be considered below.

The stratigraphic scheme of the BC boreholes is reported in Fig. 3 together with the nearby sites of A14 and CA by Di Vito et al. (1998) and Marturano et al. (2009), respectively. The A14 and CA sites are close to the seven boreholes of the Project and will be considered here, focusing on the Scafati borehole data on the plain. To this latter location (Fig. 1), eastward of the study area, refers the stratigraphy (PSc) in Fig. 3 and peaty mud sediments at 5.2 and 10.8 m b.s.l. dated 4500 ± 320 and 5600 ± 130 years BP, respectively (Barra et al., 1992a). At Pompeii six boreholes were drilled along the east and westward alleys of the so-called "Insula of Casti Amanti" (location in Fig. 2). Between the 79 AD deposits and an underlying shoshonitic lava body, the sequence (CA in Fig. 3, summarized by Marturano et al.,

2009) can be subdivided into three main layers. The middle layer, at present about 25 m a.s.l., revealed the ubiquitous presence of microfossil remains, phonolitic pumice from the Mercato eruption (8890 ± 90 cal. years), glass shard and ceramic pottery remnants characteristic of the Late Neolithic Diana Culture pottery (4300–3700 BC). The pumice samples revealed a phonolitic composition with homogeneous major and trace elements typical of the "Mercato" eruption, as named by Walker (1977), also known as "Pomice Gemelle" (Delibrias et al., 1979) or "Ottaviano pumice" (Rolandi et al., 1993). The fall deposits of this eruption dispersed in an E–NE direction (e.g. Mele et al., 2010), as generally occurs for plinian and subplinian Vesuvian eruptions with the exception of that of 79 AD that deposited ash and pumice primarily to the south and southeast of the volcano. Results of micropalaeontological analysis suggested that sedimentation occurred in a high-energy marine paleoenvironment, like the upper part of the infralittoral zone, infralittoral fringe or midlittoral zone.

Di Vito et al. (1998) documented at core A14 (location in Fig. 2) low sea level sediments at about 15 (A14a) and 24 m b.s.l. (A14b) dated 18–20 ka (sequence A14 in Fig. 3, from Di Vito et al., 1998). Radiocarbon dating of the humified levels under two lava blocks of core A14 revealed age inversion: an upper palaeosol dated 20300 ± 200 BP and lower palaeosol dated 18700 ± 280 BP (Di Vito et al., 1998). The age inversion of palaeosoils is generally a crucial point for analysis of stratigraphic sequences. The large error used below overcomes the obstacle as it permits confirmation of the average uplift rate for longer, which is the goal of this article. However, anomalous age patterns through sediment cores are not rare, particularly when ^{14}C dating is performed on organic matter dispersed in sediments with a complex accumulation history (Di Vito et al., 1998). Therefore, caution is required in interpreting core A14 (Di Vito et al., 1998; Milia et al., 2008). The two dates, calibrated to calendar years with the IntCal104 dataset (Reimer et al., 2004), are 22.7 and 24.7 cal. kyr BP, older than the volcanic bodies overlying the palaeosoils, and therefore, according to petrographical features of the lava flows, consistent with their emplacement preceding the Pomice di Base-Pomice Verdoline activity (22–19 cal. kyr BP; Santacroce and Sbrana, 2003; Di Renzo et al., 2007; Santacroce et al., 2008).

As reported in the previous section, pre-79 AD marine sediments at BC holes are situated from 8 down to –24 m a.s.l., characterized by microfossil assemblages indicating shallow marine palaeoenvironments. Marine sediments at comparable depth are also reported in sequence A14 (Fig. 3), where the elevation of the ^{14}C dated samples (ellipses) is also indicated.

Recently, Lambeck et al. (2004), Lambeck and Purcell (2005), Pirazzoli (2005) and Stocchi and Spada (2008) evaluated the components combining to produce sea level change after the last deglaciation and developed a predictive model for Late Pleistocene and Holocene changes in relative sea level for the Italian coast. They concluded that relative sea level is spatially variable along the Italian peninsula and across its adjacent seas due to glacio-hydro-isostatic effects, and sea level cannot be represented by a single time-dependent curve for the entire region. Their results primarily reveal coastal stability along the Tyrrhenian coast since the middle Pleistocene, using the position of the MIS 5.5 horizon as marker (Lambeck et al., 2004; Antonioli et al., 2009). Absolute sea level change (solid curve in Fig. 4) is plotted by smoothing with a ninth-order polynomial the reconstruction by Lambeck et al. (2010).

According to Marturano et al. (2009), the solid line passing through point CA represents the CA site-level change from the sediment deposition (~7.5 kyr) to the present position (25 m a.s.l.), showing an average uplift rate of ~5 mm/yr. In Fig. 4 A14 sediments are also plotted at the present (A: 15 m b.s.l. B: 24 m b.s.l.) and at their original location back down to the palaeoshoreline as inferred by calibrated ages (22.7 and 24.7 cal key BP). The A14 sediment

Table 2 Semiquantitative distribution of foraminifer and ostracod remains (*a* = abundant, *c* = common, *u* = uncommon, *r* = rare) and presence of further calcareous microfossils.

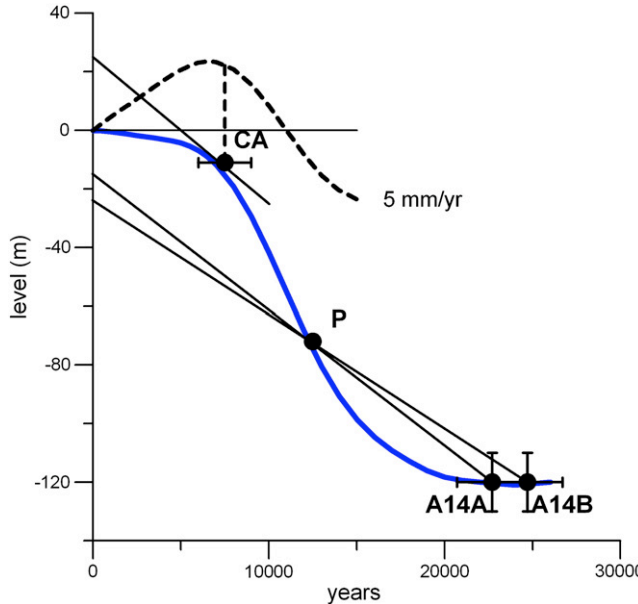


Fig. 4. Sea level change (curve) along the Campanian coast; vertical bars indicate total prediction uncertainty (Lambeck et al. 2004). The horizontal bars correspond to age range for Mercato eruption (8890 ± 90 year) and Diana Late Neolithic phase (4300–3700 B.C.) for CA, and age limit for marine sediments in borehole A14 (± 2000 year). The three lines represent the relative ground movement of sites CA and A14A,B; the present day intersects at 25, −15 and −24 m a.s.l. Dashed curve and line represent, respectively, the current elevation of past shorelines at constant tectonic rates of 5 mm/year, and relative vertical movement of CA.

trajectories (lines) indicate a long period of subaerial environment up to about 13 kyr BP (P in Fig. 4), after which a marine environment is attained. The A14 calibrated ages are reported with an error of ± 2000 years to account for the data inversion. The corresponding estimated uplift rates range from 4.0 to 5.1 mm/year in accordance with the CA rate. Following this trend, A14 sediments supported a tectonic upwelling of about 100 m (Fig. 4). The vertical bars consider the total prediction uncertainty as reported by Lambeck et al. (2004).

The dashed curve in Fig. 4 represents the elevation of the past shoreline, $h(t)$, for the case of constant tectonic uplift rate (5 mm/year); the vertical dashed line the movement of sediments CA. Shoreline elevation at an uplift rate of 5 mm/year (dashed curve $h(t)$ in Fig. 4) shows that at ~11 kyr, the level at $h=0$ overtakes the curve. Any marine sediment produced at a very low depth (~0 m b.s.l.) at that time would now have zero elevation, and any older sediment would still have negative elevation. At the supposed tectonic rise (5 mm/year), the sediment with the highest possible present elevation was produced about ~7 kyr ago. Fig. 5a jointly reports sea level change (solid curve), function $h(t)$ (dashed curve), trajectories (solid lines) for P and CA (filled circles) at a 5 mm/year uplift rate and, finally, the present elevation of BC samples represented by the top (t) and bottom (b) samples for each borehole to improve legibility.

From micropalaeontological analysis of BC samples, very low marine water is inferred for long intervals of time, in spite of the contemporaneous appreciable sea level rise. The constant water level suggests a constant ground uplift rate close to that of sea level, with the joint contribution of sediment pile up and tectonic rise. The BC1 low marine water samples are located above current sea level (see also Fig. 3), which is the highest level at any time since the Last Glacial Maximum, providing evidence for uplift and deposition after 11 kyr. The other BC samples are all beside the present sea level. To determine the age of deposition of BC sediments, the present BC locations are plotted back down to the palaeoshoreline at an average rate of 5 mm/year (Fig. 5a). Vertical

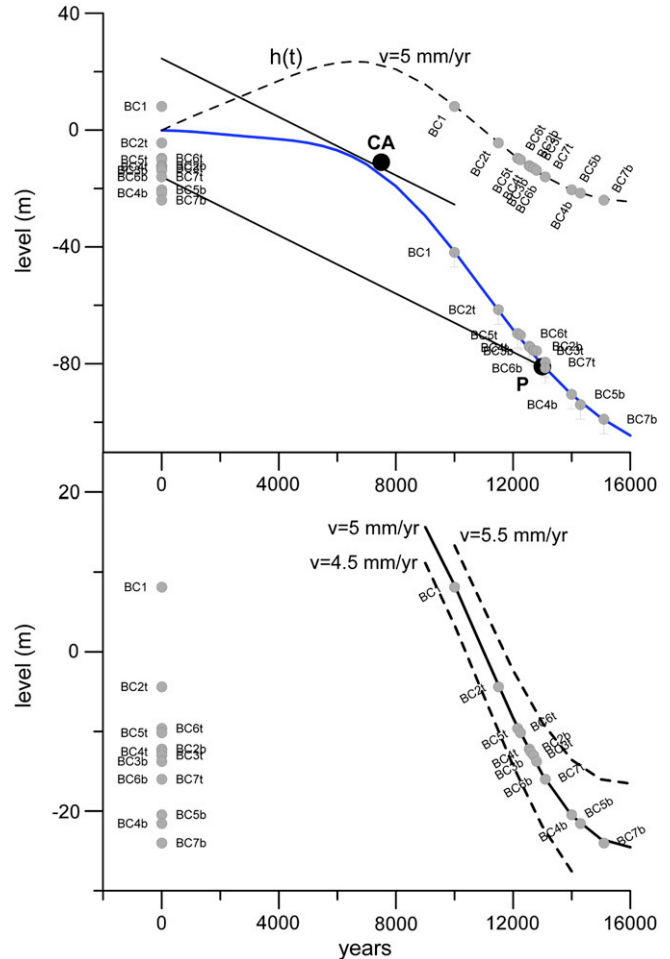


Fig. 5. a) Sea level change along the Campanian coast (continuous curve); curve $h(t)$ representing present elevation of past shoreline, assuming constant tectonic rate of 5 mm/year (dashed). Solid circles represent CA and P as in Fig. 4; open circles BC samples. b) Enlargement of part of Fig. 5a representing $h(t)$ curves at 4.5, 5.0 and 5.5 mm/year and BC samples (open circles with error bars of 5 m).

bars of −5 m are also reported in order to retain the features of low marine water (Fig. 5a).

The present elevations of BC samples are also plotted on the $h(t)$ curve (Fig. 5a) and magnified in Fig. 5b where functions $h(t)$ representing tectonic uplift rates of 4.5 and 5.5 mm/year are also reported.

4. Volcano-tectonic contribution

In theory, it is relatively straightforward to determine pre-historic vertical ground deformation on volcanoes as well as in non-volcanic areas, by utilizing absolute sea level data. In practice, determination remains problematic on volcanoes because rapid environmental changes potentially influence the printing and detention of records in the natural archives. And this makes it difficult to isolate single components unambiguously, which is essential for studies on a potentially hazardous apparatus.

Uplift and subsidence of the Earth's surface are observed in many volcanic areas. The displacement pattern reveals such characteristics as depth and rate of magma accumulation (e.g. Dvorak and Dzurisin, 1997). In addition to rapid changes associated with individual eruptions, long-term changes occur in the shape of volcanoes. Strain rates of a few millimeters/year, comparable to tectonic ones estimated in Southern Italy (1–2 mm/year; Luongo et al., 1991; Westaway, 1993; Bordini and Valensise, 1998; Amato and Cinque, 1999; Patacca and Scandone, 2001; Ferranti and Oldow, 2005), have been calculated

for volcanoes in the Tyrrhenian Sea (e.g. Lucchi et al., 2007), but strain rates of several mm/year have also been reported for volcanoes close to Vesuvius. Indeed, an uplift rate exceeding 30 mm/year for Mt Epomeo on the island of Ischia (Gillot et al., 1982; Vezzoli, 1988; Barra et al., 1992b; Carlino et al., 2009; Vezzoli et al., 2009) and in the order of 6–16 mm/year for the Holocene sediments of La Starza terrace at Pozzuoli, Campi Flegrei, have been estimated (Cinque et al., 1985; Barra, 1992; Acocella, 2008). An uplift roughly one order of magnitude greater has been recorded at Yasur Volcano (~150 mm/year), Tanna Island, Vanuatu Island Arc (Chen et al., 1995; Neef et al., 2003) and Iwo-Jima Island (150–200 mm/year), Izu-Bonin Arc (Kaizuka, 1992), and finally an uplift rate of 800–1000 mm/year have been observed at Campi Flegrei in seventy and eighty years of last century, the last being the highest uplift rate among the known caldera volcanoes in the world (Corrado et al., 1976; Barberi et al., 1984; De Natale et al., 2006a).

The Somma-Vesuvius volcano has experienced both single eruption upwelling of some metres, and long-term ground deformation at a rate of 5 mm/yr for the last several kyr (Marturano, 2008; Marturano et al., 2009). The A14 deep marine sediments experienced ~100 m of uplift from the late Pleistocene at a rate of 5 mm/year extending back in the time the previously estimated uplift rate. Following the volcanoclastic sequence, i.e. marine sands separated by a palaeosol (Di Vito et al., 1998), it is proposed that deposits at A14 log experienced subaerial uplift conditions up to ~13 kyr by utilizing a linear trend (Figs. 4 and 5). Consequently, samples drilled by BC logs can be relatively dated confirming that marine succession unconformably covered older sediments. It is to be emphasized that more sophisticated uplift trends are not justified by poor available data. We suppose that the vertical uplift is of a volcanotectonic nature and that the contribution of regional tectonics is negligible, appearing to be one order of magnitude smaller (e.g. Brancaccio et al., 1991; Ferranti and Oldow, 2005).

A Maxwell viscoelastic behaviour with varying rheological parameters may be appropriate for the bulk of the crust underlying the volcano (Zollo et al., 1998; Nunziata et al., 2006; Cubellis et al., 2007). However, fine scale details in load history and local variations in crustal rheology remain poorly known. We rely therefore on simplified earth models with uniform rheology. A deep source of strain located in an elastic half space produces displacement of the surface as shown in Fig. 6a. If we consider a surface line S and the source C as the only source of strain, the temporal change of surface morphology can be represented by the curves S_0, \dots, S_5 at times $t_0 < \dots < t_5$ (Fig. 6b): note the vertical displacement of the surfaces and the horizontal shifting of lower parts (arrows in figure). In order to simulate the deformation of the apron of our volcano and the Sarno Valley, we consider a dislocation model, like a horizontal sheet, based on the formulas of Okada (1992). The source, 20–25 km deep, corresponding to the depth of the low velocity zone underlying the crust (e.g. Panza et al., 2007), is centred along the axis of the summit caldera of the volcano. The source is assumed large as the base of the volcano (20 km) and the parameters are calibrated to obtain a vertical rate of 5 mm/year at 10 km and to constrain the magma supply rate close to bibliography values and average eruption rate (Joron et al., 1987; Cioni et al., 2003 and reference therein). The calculated ~19 kyr palaeosurface environment is shown in Fig. 7a, where the present-day coastline and the Sarno River are also reported, together with the horizontal displacement of the lower parts of the valley and the supposed river course (dashed curve). In Fig. 7b the top of Campanian Ignimbrite is reported (CI; 39 ka) by Aprile and Toccaceli (2002) as possibly appearing around the Last Glacial Maximum. Vertical coincidence of the lower parts of the two valleys (dashed curves in Fig. 7a and b) supports both model and vertical rate operating for a long time. Fig. 7c reports the top of CI and the calculated surface at 19 kyr. The two surfaces, around Scafati, appear ~30 m distant, according to the thickness of the sediments as reported

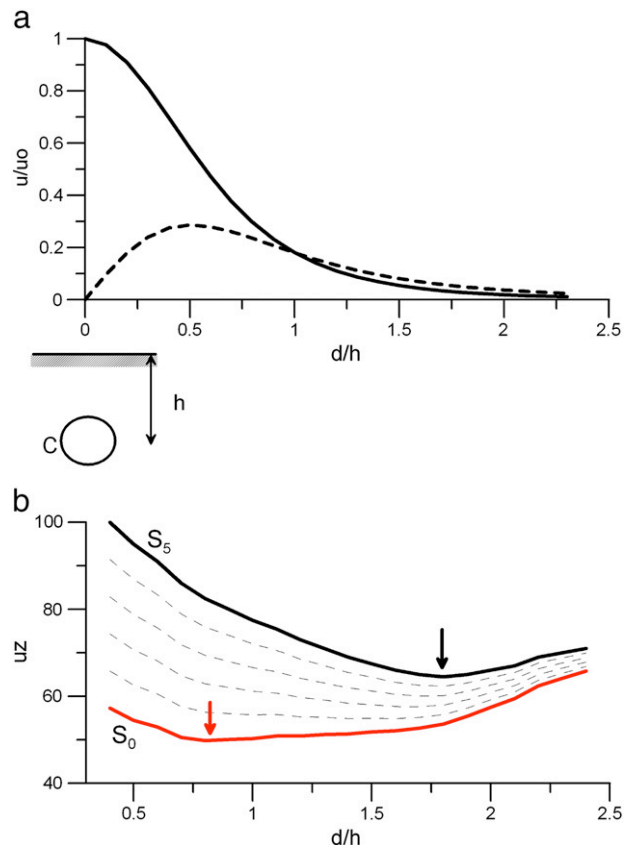


Fig. 6. a) Source of strain. Vertical (continuous) and horizontal (dashed) surface displacement produced by a source (C) of strain centred at depth h . b) displacement of surface line in time (S_0, \dots, S_5) produced by a deep source of strain: note the lateral shifting of the bottom of the surface (arrows).

by Aprile and Toccaceli, 2002. In the same figure (Fig. 7c) the vertical line joins the two surfaces at the site of the Scafati borehole. If the sediments are erased the two surfaces roughly coincide at the older age; at the intermediate age calibration is possible by using borehole data.

The Sarno Valley at present is reported in Fig. 8a. Fig. 8b proposes the palaeoenvironment of the Sarno Valley at 13 kyr BP by utilizing the data around Pompeii and Scafati. The palaeosurface is obtained by deforming the surface from the above model and lowering the valley by ~15 m as indicated by the thickness of sediments at Scafati and BC boreholes at 13 kyr. The submerged area in Fig. 8b is obtained by utilizing sea level data from Lambeck et al. (2010). Palaeocoastlines at 15 and 11 kyr inferred by BC data are represented in Fig. 9a and b. The submerged areas appear roughly the same at 15, 13 and 11 kyr although the sea level rose by ~40 m in the same period. Evidently, the tectonic and sedimentation rates, the latter around 6 m/kyr as inferred by BC samples (Figs. 3, 5 and Table 1), offset the sea level rise, leading to relative palaeoenvironmental stability in the area.

The BC boreholes do not report marine samples younger than ~9 kyr. During the Holocene several Vesuvian eruptions concerned the Sarno Valley. Among them, three main plinian eruptions, Mercato (9 ka), occurring 10 kyr after the last sub-plinian (Greenish, 19 ka), Avellino (4 ka) and Pompeii (AD 79), supplied several km³ of pyroclastic materials (e.g. Santacroce et al., 2008). Both the amount of dispersed loose pyroclastics by volcanic activity and the varying climatic conditions from the semiarid of the late Pleistocene to wetter conditions in the Holocene favoured erosion and deposition rate change (e.g. Zanchetta et al., 2004). Moreover, the relative equilibrium between land and sea level was changing: the tectonic uplift rate finally exceeded the rate of sea level rise, and, as a

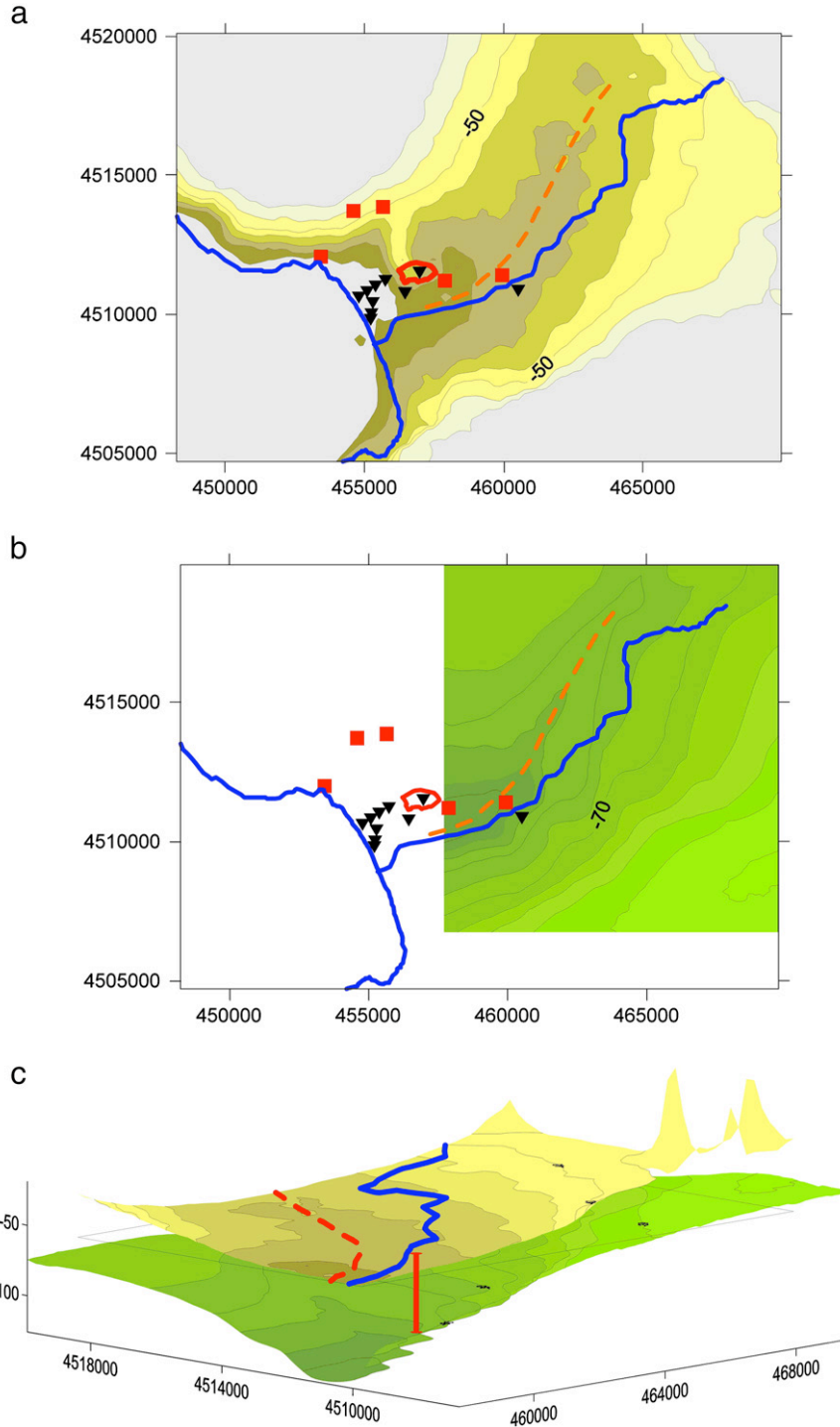


Fig. 7. Sarno Valley. a) 19 kyr palaeosurface of the Sarno Valley calculated by using a source of strain 25 km deep centred below the summit caldera of Somma-Vesuvius. b) Top of Campanian Ignimbrite (CI, by [Aprile and Toccaceli, 2002](#)). Note the correspondence of the bottom of the two valleys evidenced by dashed curves. c) Top of CI and calculated palaeosurface; the line links the location of the Scafati borehole.

consequence, part of the valley experienced erosion, partially erasing younger marine sediments. At 7 kyr the Pompeii hill had not yet re-emerged and the palaeo-Sarno joined the sea in the median part of the valley ([Fig. 9c](#)). The reconstruction in [Fig. 9c](#) is supported by CA samples and dating on peaty mud found at the Scafati borehole (6.3 cal. kyr BP).

At present, marine samples are recognized high above sea level at Pompeii and at BC1. [Cinque and Irollo \(2004\)](#) pointed out late-Pleistocene marine sediments at S. Abbondio hill (SE of ancient Pompeii, [Fig. 2](#)) and marine sediments a few metres a.s.l. have been

recognized at P33, P34, P35, P39 and P43 from previous boreholes ([Barra et al., 1992a](#)) (see locations in [Fig. 2](#)). The location of all these boreholes is on the right bank of the Sarno River, between Pompeii and the sea, supporting partial preservation of the study area from erosion processes.

5. Discussion and conclusions

The study area comprises the southwestern coastal plain of the Sarno River, between the ancient city of Pompeii and the sea. A NW-

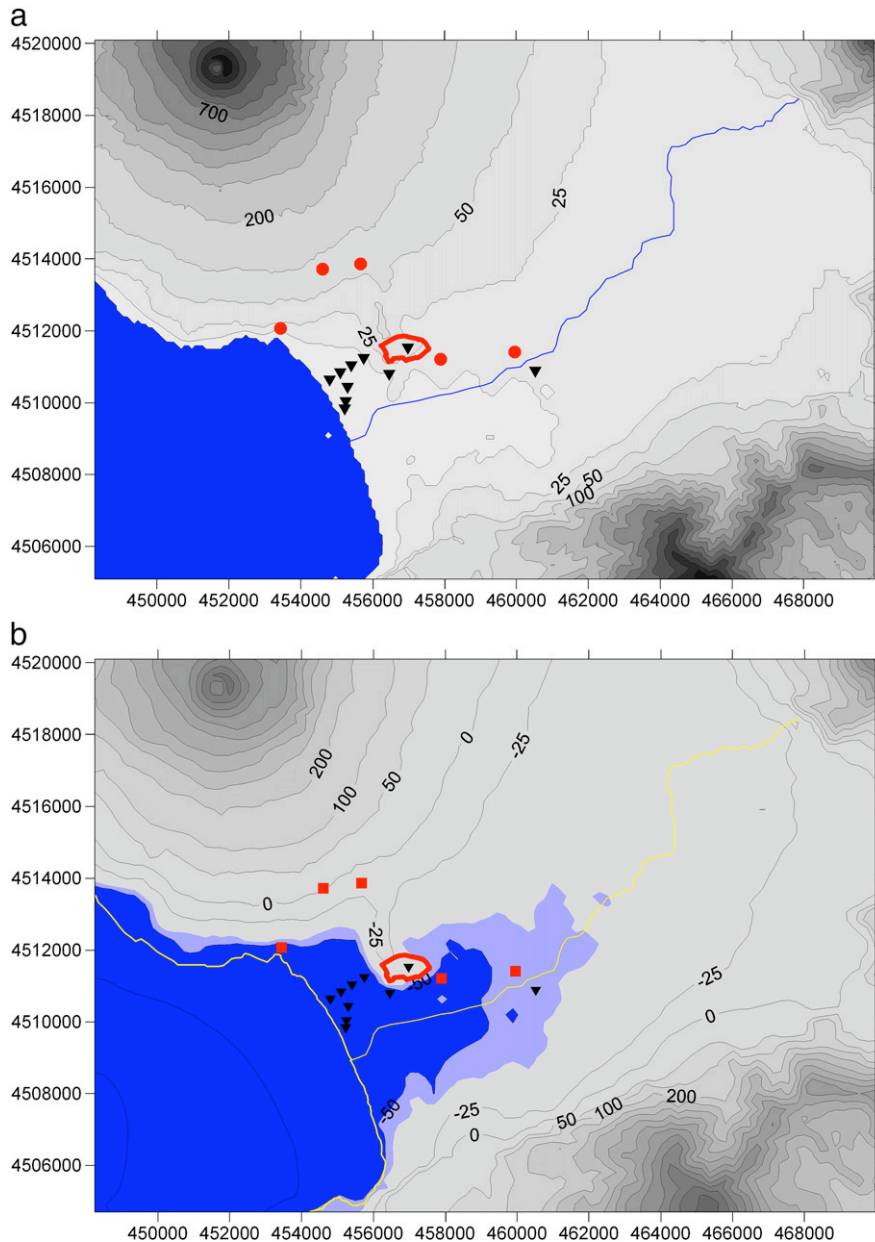


Fig. 8. Sarno Valley at present (a) and 13 kyr ago (b). The sea submerged the area of BC boreholes (blue); the low sea depth around Scafati is in light blue.

SE escarpment developing between 25 and a few m a.s.l. crosses the area: on the top is Pompeii, southwestward the other logs (Fig. 2). The escarpment has been interpreted as a Holocene palaeo-sea cliff (Cinque and Russo, 1986; Cinque, 1991; Barra et al., 1992a; Vogel and Märker, 2010), assigning to the succession at the base the last 5–7 kyr by dating at the Scafati borehole near the Sarno River. The lava flows, evident under Pompeii but drilled by A14 log, account for the elongated hill at Pompeii that runs perpendicular to the Sarno River, partially setting the emerging study area apart in the last kyr.

Importantly the Somma-Vesuvius volcanic complex and the Sarno Plain are located within a global tectonic subsidence framework of the Campanian Plain with respect to the bordering carbonates and present a complex pattern of faults with normal and strike-slip kinematics (e.g. Patacca et al., 1990; Luongo et al., 1991; Bruno et al., 1998; Brocchini et al., 2001; Milia et al., 2003a,b; Aiello et al., 2005; Piochi et al., 2005). However, the seismicity of the area is low, and

shows no links with tectonic alignments (e.g. De Natale et al., 2001; Cubellis et al., 2007; Galluzzo et al., 2008). Nor have recent aseismic displacements on the fault been detected. The seismicity recently recorded is marked by events at Vesuvius with a frequency of a few hundred per year concentrated in the summit caldera ($M_D \leq 3.6$) at a depth of less than 6 km below sea level (e.g. Vilardo et al., 1996; Bianco et al., 1999; Capuano et al., 1999; Cubellis and Marturano, 2002; Zollo et al., 2002; De Natale et al., 2004, 2006b; Galluzzo et al., 2008). According to pre-instrumental seismicity data in modern times, the most severe events took place in 1794 and prior to the eruption of 1631 ($M \approx 4.5$) (e.g. Cubellis and Marturano, 2002; Principe et al., 2004; Bertagnini et al., 2006). In Classical times the largest earthquake, the AD 62 $M = 5.1 \pm 0.3$ event, occurred during the uplift of the volcanic apparatus preceding the 79 AD eruption (Mercalli, 1883; Marturano and Rinaldis, 1995; Boschi et al., 1997; Marturano, 2008). In sum, given the low seismicity rate, seismic-

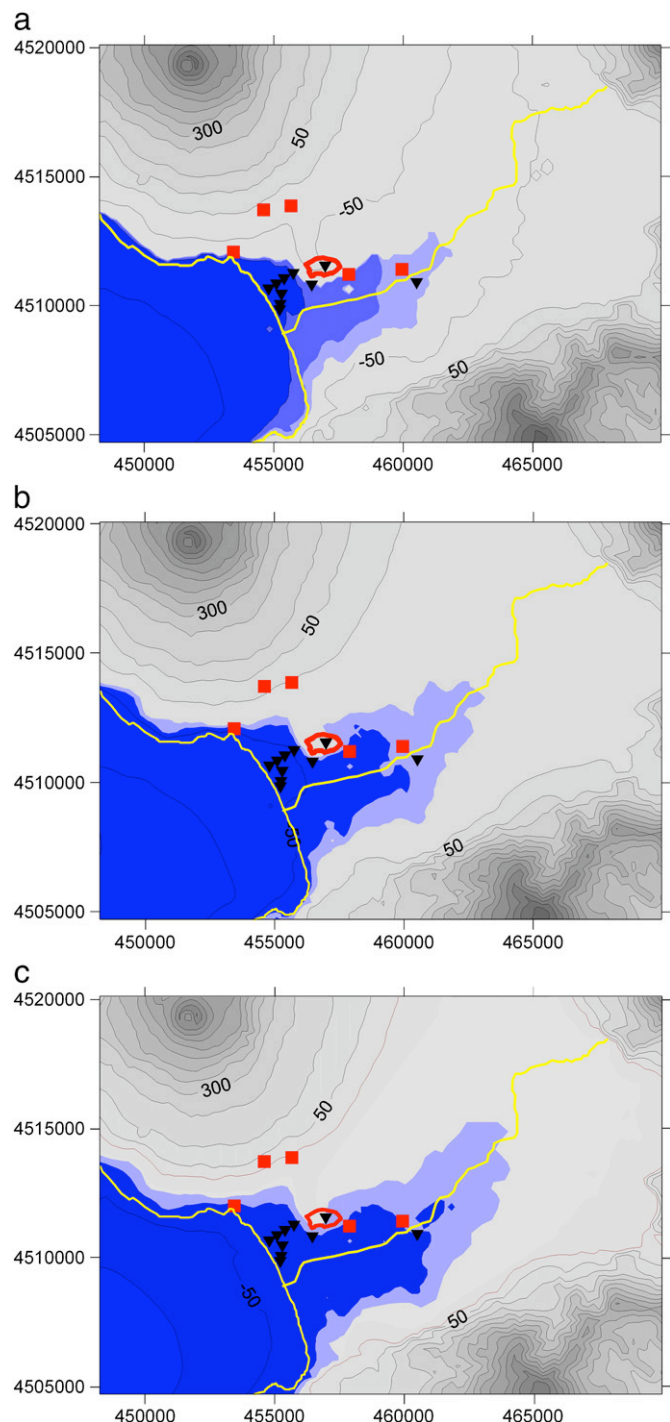


Fig. 9. Sarno Valley at 15 (a), 11 (b) and 7 kyr (c).

related tectonic motion can be judged negligible, and the long-term average uplift is a useful quantity to represent the dynamic of the area unaffected by abrupt offset.

In coastal areas tsunamis should also be taken into account to correctly interpret borehole data. Tsunamis can be of seismic or volcanic origin. The Italian Tsunami Catalogue does not report the dangerous effects of tsunamis for the Bay of Naples linked to earthquakes for the last three centuries, the completeness period, or two millennia, the time interval spanned by the catalogue (Tinti et al., 2004).

Tsunamis of volcanic origin can be caused by the impact of pyroclastic flows or surges, submarine explosions, flank or caldera

collapse (e.g. Blong 1984). The Ischia and Campi Flegrei volcanoes, seamounts and volcanoes of the Aeolian Arc in the Southern Tyrrhenian Sea are possible sources of potentially dangerous tsunamis for the Bay of Naples. Pyroclastic flows or surges are known to accompany all the large eruptions occurring at Ischia (~55 ka Mount Epomeo Green Tuff) and Campi Flegrei (39 ky Campanian Ignimbrite and 15 ky Neapolitan Yellow Tuff) (e.g. Barberi et al., 1978; Vezzoli, 1988; De Vivo et al., 2001; Deino et al., 2004; Tibaldi and Vezzoli, 2004; Brown et al., 2007; Santacroce et al., 2008; Carlino et al., 2009). Moreover, sector collapses were proposed for Stromboli, the Aeolian Isles (Kokelaar and Romagnoli, 1995) and Ischia (Chiocci and de Alteriis, 2006). Despite the data and the sources, geological proof of tsunamis along the coast (off- and onshore) between Naples and the Sorrento Peninsula has not been reported. Although large volumes of pyroclastic and debris flows entering the sea are considered tsunamigenic (e.g. Mattioli et al., 2007), the potential generation and effects of tsunami produced by flows travelling down the flank of Somma-Vesuvius is a matter for debate. Deposits of thick debris avalanches and pyroclastic currents offshore of Somma-Vesuvius associated with the Pomice di Base, Avellino Pumice and AD 79 eruptions of Vesuvius were recently recognized (Milia et al., 2003a,b, 2007, 2008). On the contrary, field evidence discards lateral collapses of the volcano in the last 20000 years (Cioni et al., 2008) and the calculated size of tsunamis generated by data on pyroclastic flows of a big eruption at Vesuvius, like AD 79, appears modest (<1 m) (Tinti et al., 2003). Nevertheless, these issues would be worth investigating for hazard evaluation in management of coastal zones (e.g., Milia et al., 2008).

However, catastrophic events produce unusual layers in prevailing deposits in the sedimentary sequence, and the related micropalaeontological assemblages should show some evidence of resedimentation (e.g. mixed assemblages, dimensional selection, abraded tests and valves). Conversely, our micropalaeontological analysis evidenced autochthonous assemblages, and the resulting data constrained the palaeosea depth to constant values for a broad time range and led to extreme events like high magnitude storms and tsunamis being rejected.

The previous detected rise was restricted to the "Insula of Casti Amanti" on the lava hill of ancient Pompeii. On this ground Marturano et al. (2009) did not exclude a very local cause, although involvement of the whole Somma-Vesuvius structure was reasonably assumed. The new data extending the uplift area strengthen the latter hypothesis.

There is the further interesting question regarding the use of palaeoenvironmental results. From micropalaeontological analyses, very low marine water is inferred for long intervals of time, in spite of appreciable sea level rise. Constant palaeobathymetric data suggest a constant ground uplift rate close to sea-level rise, providing an insight into the long-term dynamic evolution of the volcano. Indeed, taking this characteristic into account, a tectonic uplift rate close to 5 mm/year can be confirmed up to ~15 kyr BP. In this lapse of time the sea level rose ~90 m, the land 75 m and marine sediments accumulated at ~6 m/kyr.

Interestingly, the sedimentary sequence is not interrupted by large amounts of abrupt pyroclastic depositions excluding the primary role of large explosive eruptions around the stable low-sea. On the contrary, our observations suggest that volcano-tectonics played an important role in forming the geomorphology of the apron area near Pompeii. In Fig. 10 a NE-SW cross-section from Pompeii to the sea is reported (dashed section in Fig. 2). Settings at the present time, ~7 and ~13 kyr ago, evidence a well-defined pattern of uplift in accordance with sea level changes. In Fig. 10 the present-day morphology is reported shaded in the other two sketches at 7 and 13 kyr, as also reporting the marine sediment elevation (stars) and depth of the holes. At ~7 and ~13 kyr the sea level was, respectively, around 10 and 70 m lower than the present day.

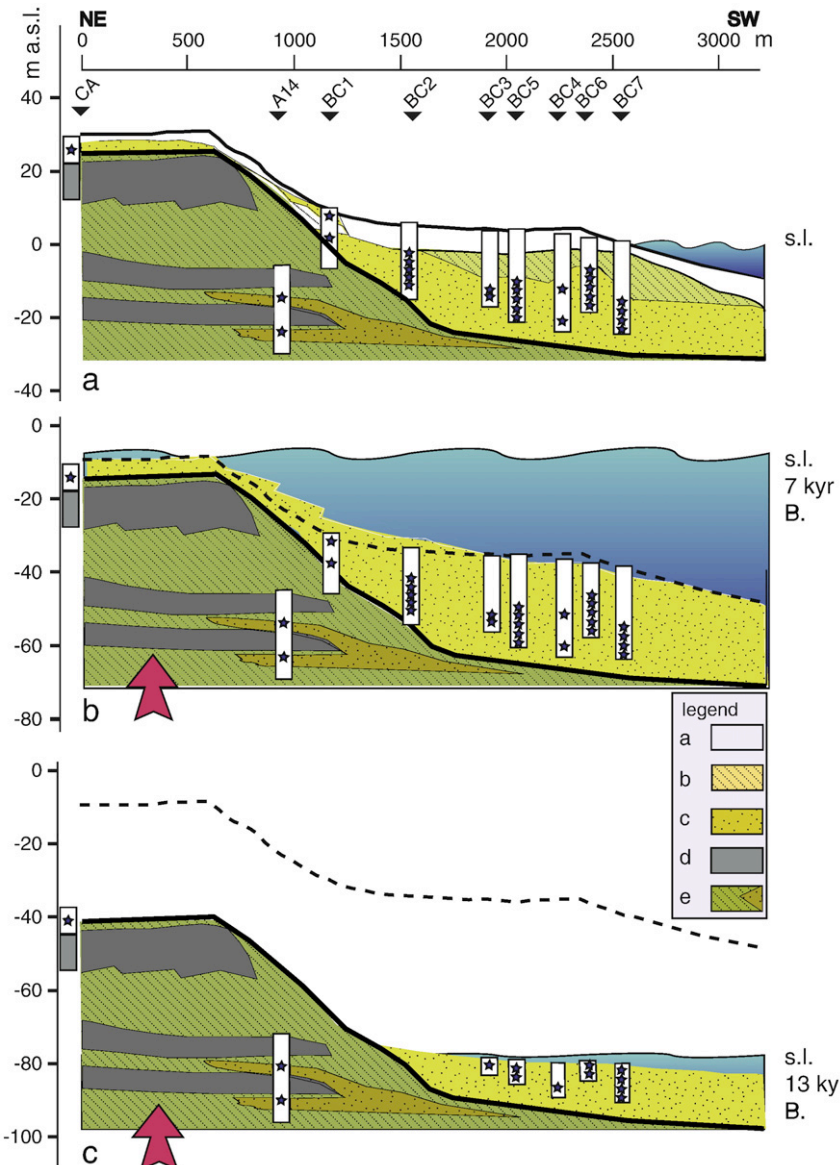


Fig. 10. Cross-section from Pompeii to the sea (location in Fig. 2) at present (a), ~7 kyr (b) and ~13 kyr (c). Marine fossiliferous sediments (stars) and location of the boreholes are reported. The sea level at ~7 and ~13 kyr is ~10 m and ~70 m b.s.l respectively (Lambeck et al., 2004). Legend: a) 79 AD pyroclastic flow and fall and post 79 AD reworked deposits; b) sands and reworked deposits; c) lava flow, block lavas and scoria; c) marine; d) sands, reworked and marine sediments.

The samples above the sea level, as well as BC1, CA (at ancient Pompeii), at S. Abbondio, P33, P34, P35, P39 and P43, (Fig. 2) evidence that edges of marine sediments escaped erosion following emergence of the area. Indeed, during the time interval recorded by the studied sequence shown in Fig. 10, the sea rose but at a progressively decreasing rate until ground uplift prevailed. Consequently, the coastal features underwent changes and erosional features prevailed over those of deposition.

Finally, during the early Holocene the sea flooded the Pompeian lava hill. Our new findings have shifted further upward and northward the previously supposed limit to Holocene marine ingressions (e.g. Barra et al., 1992a). Just beyond that limit a Neolithic human community was to settle and provide the first evidence for the onset of new emergence.

Acknowledgments

We are grateful for the constructive reviews of two anonymous reviewers and the editor Lionel Wilson that is warmly thanked.

Appendix A. List of species

Foraminiferida

- (1) *Adelosina elegans* (Williamson)=*Miliolina bicornis* (Walker) var. *elegans* Williamson, 1858
- (2) *Adelosina longirostra* (d'Orbigny)=*Quinqueloculina longirostra* d'Orbigny, 1826
- (3) *Adelosina mediterranensis* (Le Calvez and Le Calvez)=*Quinqueloculina mediterranensis* Le Calvez and Le Calvez, 1958
- (4) *Ammonia gaimardi* (d'Orbigny)=*Rotalia (Turbuline) gaimardi* d'Orbigny, 1826
- (5) *Ammonia parkinsoniana* (d'Orbigny)=*Rosalina parkinsoniana* d'Orbigny, 1839
- (6) *Ammonia perlucida* (Heron-Allen and Earland)=*Rotalia perlucida* Heron-Allen and Earland, 1913
- (7) *Ammonia tepida* (Cushman)=*Rotalia beccarii* (Linneo) var. *tepida* Cushman, 1926

- (8) *Asterigerinata mamilla* (Williamson) = *Rotalina mamilla* Williamson, 1858
 (9) *Astrononion stelligerum* (d'Orbigny) = *Nonionina stelligera* d'Orbigny, 1839
 (10) *Bolivina striatula* Cushman, 1922
 (11) *Buccella granulata* (Di Napoli Alliata) = *Eponides frigidus granulatus* Di Napoli Alliata, 1952
 (12) *Bulimina aculeata* d'Orbigny, 1826
 (13) *Bulimina elongata* d'Orbigny, 1846
 (14) *Cibicides lobatulus* (Walzer and Jacob) = *Nautilus lobatulus* Walzer and Jacob, 1798
 (15) *Cornuspira involvens* (Reuss) = *Operculina involvens* Reuss, 1850
 (16) *Elphidium complanatum* (d'Orbigny) = *Polystomella complanata* d'Orbigny, 1939
 (17) *Elphidium crispum* (Linneo) = *Nautilus crispus* Linneo, 1758
 (18) *Elphidium cuvillieri* Lévy, 1966
 (19) *Elphidium incertum* (Williamson) = *Polystomella umbilicatula* (Walker) var. *incerta* Williamson, 1858
 (20) *Elphidium granosum* (d'Orbigny) = *Nonionina granosa* d'Orbigny, 1846
 (21) *Elphidium macellum* (Fichtel and Moll) = *Nautilus macellus* Fichtel and Moll, 1798
 (22) *Elphidium pulvereum* Todd, 1958
 (23) *Elphidium punctatum* (Terquem) = *Polystomella punctata* Terquem, 1878
 (24) *Elphidium* sp. A [Sgarrella and Moncharmont Zei, 1993](#)
 (25) *Lagena clavata* (d'Orbigny) = *Oolina clavata* d'Orbigny, 1846
 (26) *Lamarckina scabra* (Brady) = *Pulvinulina oblunga* (Williamson) var. *scabra* Brady, 1884
 (27) *Massilina secans* (d'Orbigny) = *Quinqueloculina secans* d'Orbigny, 1826
 (28) *Miliolinella subrotunda* (Montagu) = *Vermiculum subrotundum* Montagu, 1803
 (29) *Nonionella turgida* (Williamson) = *Rotalina turgida* Williamson, 1858
 (30) *Planorbolina mediterranensis* d'Orbigny, 1826
 (31) *Quinqueloculina berthelotiana* d'Orbigny, 1839
 (32) *Quinqueloculina bosciana* d'Orbigny, 1839
 (33) *Quinqueloculina contorta* d'Orbigny, 1846
 (34) *Quinqueloculina lamarckiana* d'Orbigny, 1839
 (35) *Quinqueloculina lata* Terquem, 1876
 (36) *Quinqueloculina poeyana* d'Orbigny, 1839
 (37) *Quinqueloculina pygmaea* Reuss, 1850
 (38) *Quinqueloculina seminulum* (Linneo) = *Serpula seminulum* Linneo, 1758
 (39) *Quinqueloculina stalkeri* Loeblich and Tappan, 1953
 (40) *Quinqueloculina stelligera* Schlumberger, 1893
 (41) *Quinqueloculina tenuicollis* (Wiesner) = *Miliolina tenuicollis* Wiesner, 1923
 (42) *Reussella spinulosa* (Reuss) = *Verneuilina spinulosa* Reuss, 1850
 (43) *Rosalina bradyi* (Cushman) = *Discorbis globularis* d'Orbigny var. *bradyi* Cushman, 1915
 (44) *Rosalina floridana* (Cushman) = *Discorbis floridana* Cushman, 1922
 (45) *Rosalina obtusa* d'Orbigny, 1846
 (46) *Sigmoilina costata* Schlumberger, 1893
 (47) *Sigmoilina grata* (Terquem) = *Spiroloculina grata* Terquem, 1878
 (48) *Sigmoilina tenuis* (Czjzek, 1848) = *Quinqueloculina tenuis* Czjzek, 1848
 (49) *Sigmoilina tricosta* (Cushman and Todd) = *Spiroloculina tricosta* Cushman and Todd, 1944
 (50) *Siphonaperta aspera* (d'Orbigny) = *Quinqueloculina aspera* d'Orbigny, 1826
 (51) *Spirillina vivipara* Ehrenberg, 1843
 (52) *Spiroloculina excavata* d'Orbigny, 1846
 (53) *Stainforthia complanata* (Egger) = *Virgulina schreibersiana* Czjzek var. *complanata* Egger, 1893
 (54) *Textularia calva* Lalicker, 1935
 (55) *Tretomphalus concinnus* (Brady) = *Discorbina concinna* Brady, 1884
 (56) *Triloculina gibba* d'Orbigny, 1826
 (57) *Triloculina oblonga* (Montagu) = *Vermiculum oblongum*, 1803
 (58) *Triloculina plicata* Terquem, 1878
 (59) *Triloculina rotunda* d'Orbigny, 1893
 (60) *Triloculina schreibersiana* d'Orbigny, 1839
 (61) *Triloculina trigonula* (Lamarck) = *Miliolites trigonula* Lamarck, 1804

Ostracoda

- (1) *Aurila prasina* Barbeito-Gonzalez, 1971
 (2) *Aurila* sp.
 (3) *Callistocythere protracta* Ruggieri and D'Arpa, 1993
 (4) *Callistocythere* sp.
 (5) *Candonidae* Kaufmann, 1900
 (6) *Carinocythereis whitei* (Baird) = *Cythereis whitei* Baird, 1850
 (7) *Cistacythereis turbida* (G.W. Müller) = *Cythereis turbida* G.W. Müller, 1894
 (8) *Costa batei* (Brady) = *Cythereis batei* Brady, 1866
 (9) *Costa edwardsi* (Roemer) = *Cytherina edwardsi* Roemer, 1838
 (10) *Cytheretta adriatica* Ruggieri, 1952
 (11) *Cytheretta subradiosa* (Roemer) = *Cytherina subradiosa* Roemer, 1838
 (12) *Eucytherura angulata* G.W. Müller, 1894
 (13) *Eucytherura complexa* (Brady) = *Cythere complexa* Brady, 1866
 (14) *Hemicytherura defiorei* Ruggieri, 1953
 (15) *Hemicytherura gracilicosta* Ruggieri, 1953
 (16) *Hemicytherura* sp.
 (17) *Heterocythereis voraginosa* Athersuch, 1979
 (18) *Leptocythere bituberculata* Bonaduce et al., 1976
 (19) *Leptocythere levigata* (G.W. Müller) = *Cythere levigata* G.W. Müller, 1894
 (20) *Leptocythere macella* Ruggieri, 1975
 (21) *Leptocythere ramosa* (Rome) = *Cythere ramosa* Rome, 1942
 (22) *Loxoconcha affinis* (Brady) = *Normania affinis* Brady, 1866
 (23) *Loxoconcha ovulata* (O.G. Costa) = *Cytherina ovulata* O.G. Costa, 1853
 (24) *Microcytherura fulva* (Brady and Robertson) = *Cytherura fulva* Brady and Robertson, 1874
 (25) *Neocytherideis subulata* (Brady, 1868) = *Cytherideis subulata* Brady, 1867
 (26) *Neonesidea* sp.
 (27) *Palmococoncha turbida* (G.W. Müller) = *Loxoconcha turbida* G.W. Müller, 1912
 (28) *Paradoxostoma triste* G.W. Müller, 1894
 (29) *Paradoxostoma versicolor* G.W. Müller, 1894
 (30) *Pontocypris pellucida* G.W. Müller, 1894
 (31) *Pontocythere turbida* (G.W. Müller) = *Cytheridea turbida* G.W. Müller, 1894
 (32) *Propontocypris* sp.
 (33) *Pseudocytherura* aff. *P. strangulata* Ruggieri, 1991
 (34) *Sahnicythere* sp.
 (35) *Sclerochilus levigata* G.W. Müller, 1894
 (36) *Sclerochilus* sp.
 (37) *Semicytherura acuticostata* (Sars) = *Cytherura acuticostata* Sars, 1866
 (38) *Semicytherura* aff. *S. diafora* Barbeito-Gonzalez, 1971
 (39) *Semicytherura dispar* (G.W. Müller) = *Cytherura dispar* G.W. Müller, 1894
 (40) *Semicytherura incongruens* (G.W. Müller) = *Cytherura incongruens* G.W. Müller, 1894

- (41) *Semicytherura mediterranea* (G.W. Müller) = *Cytherura mediterranea* G.W. Müller, 1894
- (42) *Semicytherura paradoxa* (G.W. Müller) = *Cytherura paradoxa* G.W. Müller, 1894
- (43) *Semicytherura aff. S. paradoxa* (G.W. Müller, 1894)
- (44) *Semicytherura rarecostata* Bonaduce et al., 1976
- (45) *Semicytherura stilifera* Bonaduce et al., 1976
- (46) *Semicytherura sulcata* (G.W. Müller) = *Cytherura sulcata* G.W. Müller, 1894
- (47) *Semicytherura* sp.
- (48) *Tenedocythere prava* (Baird) = *Cythere prava* Baird, 1850
- (49) *Urocythereis flexicauda* Bonaduce et al., 1976
- (50) *Urocythereis margaritifera* (G.W. Müller) = *Cythereis margaritifera* G.W. Müller, 1894
- (51) *Xestoleberis communis* G.W. Müller, 1894
- (52) *Xestoleberis dispar* G.W. Müller, 1894
- (53) *Xestoleberis* aff. *X. labiata* Brady and Robertson, 1874
- (54) *Xestoleberis* sp.

References

- Acocella, V., 2008. Activating and reactivating pairs of nested collapses during caldera forming eruptions: Campi Flegrei (Italy). *Geophys. Res. Lett.* 35, L17304. doi:10.1029/2008GL035078.
- Acocella, V., Funiciello, R., 2006. Transverse systems along the extensional Tyrrhenian margin of central Italy and their influence on volcanism. *Tectonics* 25, TC2003. doi:10.1029/2005TC001845.
- Aiello, G., Angelino, A., D'Argenio, B., Marsella, E., Pelosi, N., Ruggieri, S., Siniscalchi, A., 2005. Buried volcanic structures in the Gulf of Naples (Southern Tyrrhenian Sea, Italy) resulting from high resolution magnetic survey and seismic profiling. *Ann. Geophys.* 48 (6), 883–897.
- Aiello, G., Barra, D., Coppa, M.G., Valente, A., Zeni, F., 2006. Recent infralittoral Foraminifera and Ostracoda from the Porto Cesareo Lagoon (Ionian Sea, Mediterranean). *Boll. Soc. Paleontologica Ital.* 45 (1), 1–14.
- Albore Livadie, C., Barra, D., Bonaduce, G., Brancaccio, L., Cinque, A., Ortolani, F., Pagliuca, S., Russo, F., 1991. Evoluzione geomorfologica, neotettonica e vulcanica della piana costiera del fiume Sarno (Campania) in relazione agli insediamenti anteriori all'eruzione del 79 d.C. PACT. Vulcanismo, Paleogeografia e Archeologia. Centro Univ. Beni Culturali Ravello, pp. 237–256.
- Amato, A., Cinque, A., 1999. Erosional landsurfaces of the Campano-Lucano Apennines (S. Italy): genesis, evolution, and tectonic implications. *Tectonophysics* 315, 251–267.
- Antonioli, F., Ferranti, L., Fontana, A., Amorosi, A., Bondesan, A., Braitenberg, C., Dutton, A., Fontolan, G., Furlani, S., Lambeck, K., Mastronuzzi, G., Monaco, C., Spada, G., Stocchi, P., 2009. Holocene relative sea-level changes and vertical movements along the Italian and Istrian coastlines. *Quatern. Int.* 206, 102–133. doi:10.1016/j.quaint.2008.11.008.
- Aprile, F., Toccaceli, R.M., 2002. Nuove conoscenze sulla stratigrafia e distribuzione dei depositi ignimbritici quaternari nel sottosuolo della Piana del Sarno (Salerno, Campania) – Italia Meridionale. *Quaternario* 15, 169–174.
- Arbulà, D., Pugliese, N., Russo, A., 2001. Ostracodi del Golfo Saline (Sardegna nord-orientale). *Studi Trentini Sci. Nat. Acta Geol.* 77, 25–35.
- Arbulà, D., Pugliese, N., Russo, A., 2004. Ostracods from the National Park of La Maddalena Archipelago (Sardinia, Italy). *Boll. Soc. Paleontologica Ital.* 43 (1–2), 91–99.
- Barbeito-Gonzalez, P.J., 1971. Die Ostracoden des Küstenbereiches von Naxos (Griechenland) und ihre Lebensbereiche. *Mitt. hamburgischen zoologischen Mus. Inst.* 67, 255–326 47 pls.
- Barberi, F., Innocenti, F., Lirer, L., Munno, R., Pescatore, T.S., Santacroce, R., 1978. The Campanian Ignimbrite: a major prehistoric eruption in the Neapolitan area (Italy). *Bull. Volcanol.* 41, 10–22.
- The 1982–1984 Bradyseismic crisis at Phlegraean Fields (Italy). In: Barberi, F., Hill, D.P., Innocenti, F., Luongo, G., Treuil, M. (Eds.), *Bull. Volcanol.* 47, pp. 173–411.
- Barra, D., 1992. Studio del Pleistocene superiore-Olocene delle aree vulcaniche campane. In: De Frede (Ed.), *Tesi di Dottorato di Ricerca in "Geologia del Sedimentario"*. Università degli Studi di Napoli "Federico II", Napoli. 298 pp, 9 pls.
- Barra, D., Bonaduce, G., Brancaccio, L., Cinque, A., Ortolani, F., Pagliuca, S., Russo, F., 1989. Evoluzione geologica olocenica della piana costiera del Fiume Sarno (Campania). *Mem. Soc. Geol. Ital.* 42, 255–267.
- Barra, D., Bonaduce, G., Brancaccio, L., Cinque, A., Ortolani, F., Pagliuca, S., Russo, F., 1992a. Evoluzione geologica olocenica della piana costiera del Fiume Sarno (Campania). *Mem. Soc. Geol. Ital.* 42, 255–267.
- Barra, D., Cinque, A., Italiano, A., Scorziello, R., 1992b. Il Pleistocene superiore marino di Ischia: paleoecologia e rapporti con l'evoluzione tettonica recente. *Studi Geol. Camerti* 1992/1, 231–243.
- Bertagnini, A., Cioni, R., Guidoboni, E., Rosi, M., Neri, A., Boschi, E., 2006. Eruption early warning at Vesuvius: The A.D. 1631 lesson. *Geophys. Res. Lett.* 33, L18317. doi:10.1029/2006GL027297.
- Bianco, F., Castellano, M., Milano, G., Vilardo, G., Ferrucci, F., Gresta, S., 1999. The seismic crises at Mt.Vesuvius during 1995 and 1996. *Phys. Chem. Earth A Solid Earth Geod.* 24 (11–12), 977–983.
- Blanc-Vernet, L., 1969. Contribution à l'étude des foraminifères de Méditerranée. Relations entre la microfaune et les sédiments; biocoénoses actuelles, thanatocoénoses Pliocènes et Quaternaires, 64. Recueil des travaux de la Station Marine d'Endoume, Marseille. 281 pp.
- Blanc-Vernet, L., Clairefond, P., Orsolini, P., 1979. Les foraminifères. In: Burolet, P.F., Clairefond, P., Winnock, E. (Eds.), *La mer Pélagienne: Géologie Méditerranée*, 6 (1), pp. 171–209.
- Blong, R.J., 1984. *Volcanic Hazards*. Academic Press. 424 pp.
- Bonaduce, G., Ciampo, G., Masoli, M., 1976. Distribution of Ostracoda in the Adriatic Sea. *Pubbl. Stn. Zool. Napoli* 40 (supplemento 1), 1–304.
- Bonaduce, G., Masoli, M., Pugliese, N., 1977. Ostracodi bentonici dell'alto Tirreno. *Studi Trentini Sci. Nat. Biol.* 54, 243–261.
- Bonaduce, G., Masoli, M., Pugliese, N., 1988. Remarks on the Benthic Ostracoda on the Tunisian Shelf. In: Hanai, T., Ikeya, N., Ishizaki, K. (Eds.), *Evolutionary biology of Ostracoda: its fundamentals and applications*. Proceedings of the Ninth International Symposium on Ostracoda, held in Shizuoka, Japan 29 July–2 August 1985: Developments in Palaeontology and Stratigraphy, 11, pp. 449–466.
- Bordoni, P., Valensise, G., 1998. Deformation of the 125 ka marine terrace in Italy: tectonic implications. In: Stewart, I.S., Vita Finzi, C. (Eds.), *Late Quaternary Coastal Tectonics*, 146. *Geol. Soc. Lond.*, London, pp. 71–110.
- Boschi, E., Guidoboni, E., Ferrari, G., Valensise, G., Gasparini, P., 1997. Catalogo dei Forti Terremoti in Italia dal 461 A.D. al 1990. ING-SGA.
- Brancaccio, L., Cinque, A., Romano, P., Rosskopf, C., Russo, F., Santangelo, N., Santo, A., 1991. Geomorphology and neotectonic evolution of a sector of the Tyrrhenian and of the Southern Apennines (Region of Naples, Italy). *Z. Geomorph.* N F 82, 47–58.
- Breman, E., 1976. *The Distribution of Ostracodes in the Bottom Sediments of the Adriatic Sea*. Academisch Proefschrift. 165 pp. Vrije Universiteit te Amsterdam, Amsterdam.
- Brocchini, D., Principe, C., Castradori, D., Laurenzi, M.A., Gorla, L., 2001. Quaternary evolution of the southern sector of the Campanian Plain and early Somma-Vesuvius activity: insights from the Trecase 1 well. *Mineral. Petrol.* 73, 67–91.
- Brown, R.J., Orsi, G., de Vita, S., 2007. New insights into Late Pleistocene explosive volcanic activity and caldera formation on Ischia (southern Italy). *Bull. Volcanol.* doi:10.1007/s00445-007-0155-0.
- Bruno, P.P.G., Cippitelli, G., Rapolla, A., 1998. Seismic study of the Mesozoic carbonate basement around Mt. Somma-Vesuvius, Italy. *J. Volcanol. Geotherm. Res.* 84, 311–322.
- Capuano, P., Coppa, U., De Natale, G., Di Sena, F., Godano, C., Troise, C., 1999. A detailed analysis of some local earthquakes at Somma-Vesuvius. *Ann. Geophys.* 42 (3), 391–406.
- Carlino, S., Cubellis, E., Luongo, G., Obrizzo, F., 2009. On the mechanics of caldera resurgence of Ischia Island (southern Italy). In: Troise, C., De Natale, G., Kilburn, C. (Eds.), *Mechanisms of activity and unrest at large Calderas*. Geological Society, London, pp. 181–193. Special Publications, 269.
- Chen, J.H., Taylor, F.W., Edwards, R.L., Cheng, H., Burr, G.S., 1995. Recent emerged reef terraces of the Yenkahe resurgent block, Tanna, Vanuatu: implications for volcanic, landslide and tsunami hazards. *J. Geol.* 103, 577–590.
- Chiocci, F.L., de Alteris, G., 2006. The Ischia debris avalanche. First, clear submarine evidence in the Mediterranean of a volcanic island pre-historic collapse. *Terra Nova* 18, 202–209.
- Ciarallo, A., Pescatore, T., Senatore, M.R., 2003. Su un antico corso d'acqua a nord di Pompei. *Riv. Studi Pompeiani* 14, 273–283.
- Cinque, A., 1991. La trasgressione Versiliana nella piana del Sarno (Campania). *Geogr. Fis. Dinam. Quat.* 14, 63–71.
- Cinque, A., Irollo, G., 2004. Il "Vulcano di Pompei": nuovi dati geomorfologici e stratigrafici. *Quaternario* 17, 101–116.
- Cinque, A., Russo, F., 1986. La linea di costa del 79 d. C. fra Oplonti e Stabiae nel quadro dell'evoluzione olocenica della Piana del Sarno (Campania). *Boll. Soc. Geol. Ital.* 105, 111–121.
- Cinque, A., Rolandi, G., Zamparelli, V., 1985. L'estensione dei depositi marini olocenici nei Campi Flegrei in relazione alla vulcano-tettonica. *Bull. Soc. Geol. Ital.* 104, 327–348.
- Cinque, A., Patacca, E., Scandone, P., Tozzi, M., 1993. Quaternary kinematic evolution of the Southern Apennines. Relationships between surface geological features and deep lithospheric structures. *Ann. Geofis.* 36 (2), 249–259.
- Cioni, R., Longo, A., Macedonio, G., Santacroce, R., Sbrana, A., Sulpizio, R., Andronico, D., 2003. Assessing pyroclastic fall hazard through field data and numerical simulations: example from Vesuvius. *J. Geophys. Res.* 108 (B2). doi:10.1029/2001JB000642.
- Cioni, R., Bertagnini, A., Santacroce, R., Andronico, D., 2008. Explosive activity and eruption scenarios at Somma-Vesuvius (Italy): toward a new classification scheme. *J. Volcanol. Geotherm. Res.* 178, 331–346. doi:10.1016/j.volgeores.2008.04.024.
- Corrado, G., Guerra, I., Lo Bascio, A., Luongo, G., Rampoldi, R., 1976. Inflation and microearthquake activity of Phlegraean Fields, Italy. *Bull. Volcanol.* 40 (3), 169–188.
- Cubellis, E., Marturano, A., 2002. Mt. Vesuvius: a macroseismic study of the earthquake of October 9, 1999. *J. Volcanol. Geotherm. Res.* 118, 339–351.
- Cubellis, E., Luongo, G., Marturano, A., 2007. Seismic hazard assessment at mount Vesuvius: maximum magnitude expected. *J. Volcanol. Geotherm. Res.* 162, 139–148. doi:10.1016/j.volgeores.2007.03.003.
- De Natale, G., Troise, C., Pingue, F., De Gori, P., Chiarabba, C., 2001. Structure and dynamics of Somma-Vesuvius volcanic complex. *Mineral. Petrol.* 73, 5–22.
- De Natale, G., Kuznetsov, I., Kronrod, T., Pereson, A., Saràò, A., Troise, C., Panza, G.F., 2004. Three decades of seismic activity at Mt. Vesuvius: 1972–1999. *Pure Appl. Geophys.* 161, 123–144.

- De Natale, G., Troise, C., Pingue, F., Mastrolorenzo, G., Pappalardo, L., Boschi, E., 2006a. The Campi Flegrei caldera: unrest mechanisms and hazards. In: Troise, C., De Natale, G., Kilburn, C.R.J. (Eds.), Mechanisms of Activity and Unrest at Large Calderas: Geol. Soc. London Spec. Publ. 269, pp. 25–45.
- De Natale, G., Troise, C., Pingue, F., Mastrolorenzo, G., Pappalardo, L., 2006b. The Somma-Vesuvius volcano (Southern Italy): structure, dynamics and hazard evaluation. *Earth Sci. Rev.* 74, 73–111.
- De Vivo, B., Rolandi, G., Gans, P.B., Calvert, A., Bohrson, W.A., Spera, J.F., Belkin, H.E., 2001. New constraints on the pyroclastic eruptive history of the Campanian volcanic Plain (Italy). *Mineral. Petrol.* 73, 47–65.
- Deino, A.L., Orsi, G., de Vita, S., Piochi, M., 2004. The age of the Neapolitan Yellow Tuff caldera-forming eruption (Campi Flegrei caldera, Italy) assessed by Ar-41/Ar-39 dating method. *J. Volcanol. Geotherm. Res.* 133 (1–4), 137–170.
- Delibrias, G., Di Paola, G.M., Rosi, M., Santacroce, R., 1979. La storia eruttiva del complesso vulcanico Somma Vesuvio ricostruita dalle successioni piroclastiche del Monte Somma. *Rend. Soc. Ital. Mineral. Petrol.* 35, 411–438.
- Di Renzo, M., Di Vito, M.A., Arienzo, I., Carandente, A., Civetta, L., D'Antonio, M., Giordano, F., Orsi, G., Tonarini, S., 2007. Magmatic history of Somma-Vesuvius on the basis of new geochemical and isotopic data from a deep borehole (Camaldoli della Torre). *J. Petrol.* 48, 753–784.
- Di Vito, M., Sulpizio, R., Zanchetta, G., Calderoni, G., 1998. The geology of the South Western Slopes of Somma-Vesuvius, Italy as inferred by borehole stratigraphies and cores. *Acta Vulcanol.* 10 (2), 383–393.
- Donnici, S., Serandrei Barbero, R., 2002. The benthic foraminiferal communities of the northern Adriatic continental shelf. *Mar. Micropaleontol.* 44, 93–123.
- Dvorak, J., Dzurisin, D., 1997. Volcano Geodesy: the search for magma reservoirs and the formation of eruptive vents. *Rev. Geophys.* 35, 343–384.
- Ferranti, L., Oldow, J.S., 2005. Latest Miocene to Quaternary horizontal and vertical displacement rates during simultaneous contraction and extension in the Southern Apennine orogen, Italy. *Terra Nova* 17, 209–214.
- Ferranti, L., Antonioli, F., Mauz, B., Amorosi, A., Dai Prà, G., Mastronuzzi, G., Monaco, C., Orrù, P., Pappalardo, M., Radtke, U., Renda, P., Romano, P., Sansò, P., Verrubbi, V., 2006. Markers of the last interglacial sea-level high stand along the coast of Italy: tectonic implications. *Quatern. Int.* 145–146, 30–54.
- Frezza, V., Carboni, M.G., 2009. Distribution of recent foraminiferal assemblages near the Ombrone River mouth (Northern Tyrrhenian Sea, Italy). *Rev. Micropaleontol.* 52, 43–66.
- Galluzzo, D., Zonno, G., Del Pezzo, E., 2008. Stochastic finite-fault ground-motion simulation in a wave-field diffusive regime: case study of the Mt. Vesuvius volcanic area. *Bull. Seism. Soc. Am.* 98, 1272–1288. doi:10.1785/0120070183.
- Gillot, P.-Y., Chiesa, S., Pasquare, G., Vezzoli, L., 1982. b33,000-yr K-Ar dating of the volcano-tectonic horst of the Isle of Ischia, Gulf of Naples. *Nature* 299, 242–245.
- Haake, F.W., 1977. Living benthic Foraminifera in the Adriatic Sea; influence of water depth and sediment. *J. Foraminif. Res.* 7 (1), 62–75.
- Jorissen, F.J., 1987. The distribution of benthic foraminifera in the Adriatic Sea. *Mar. Micropaleontol.* 12, 21–48.
- Jorissen, F.J., 1988. Benthic foraminifera from the Adriatic Sea; principles of phenotypic variations. *Utrecht Micropal. Bull.* 37 174 pp.
- Joron, J.L., Metrich, N., Rosi, M., Santacroce, R., Sbrana, A., 1987. Chemistry and petrography. In: Santacroce, R. (Ed.), Somma-Vesuvius. C.N.R. : Quaderni de 'La Ricerca Scientifica, 114, pp. 105–174. Rome.
- Kaizuka, S., 1992. Coastal evolution at a rapidly uplifting volcanic island: Iwo-Jima, Western Pacific Ocean. *Quatern. Int.* 15/16, 7–16.
- Kokelaar, P., Romagnoli, C., 1995. Sector collapse, sedimentation and clast population evolution at an active island-arcvolcano: Stromboli, Italy. *Bull. Volcanol.* 57, 240–262.
- Lambeck, K., Purcell, A., 2005. Sea-level change in the Mediterranean Sea since the LGM: model predictions for tectonically stable areas. *Quat. Sci. Rev.* 24, 1969–1988.
- Lambeck, K., Antonioli, F., Purcell, A., Silenzi, S., 2004. Sea-level change along the Italian coast for the past 10,000 yr. *Quat. Sci. Rev.* 23, 1567–1598.
- Lambeck, K., Antonioli, F., Anzidei, M., Ferranti, L., Leoni, G., Scicchitano, G., Silenzi, S., 2010. Sea level change along the Italian coast during the Holocene and projections for the future. *Quatern. Int.* doi:10.1016/j.quaint.2010.04.026.
- Le Calvez, J., Le Calvez, Y., 1958. Répartition des foraminifères dans la baie de Villefranche. 1-Miliolidae. *Ann. Institut Océanogr.* 35, 159–234.
- Lucchi, F., Tranne, C.A., Calanchi, N., Rossi, P.L., 2007. Late Quaternary deformation history of the volcanic edifice of Panarea, Aeolian Arc, Italy. *Bull. Volcanol.* 69, 239–257. doi:10.1007/s00445-006-0070-9.
- Luongo, G., Cubellis, E., Obrizzo, F., Petrazzuoli, S.M., 1991. A physical model for the origin of volcanism of the Tyrrhenian margin: the case of Neapolitan area. In: Luongo, G., Scandone, R. (Eds.), Campi Flegrei: J. Volcanol. Geotherm. Res., 48, pp. 173–185.
- Marturano, A., 2008. Sources of ground movement at Vesuvius before the AD 79 eruption: evidence from contemporary accounts and archaeological studies. *J. Volcanol. Geotherm. Res.* 177, 959–970. doi:10.1016/j.jvolgeores.2008.07.017.
- Marturano, A., Rinaldi, V., 1995. Il terremoto del 62 d.C. un evento carico di responsabilità. In: Dtsch. Arch. Inst. Rom. Sopr. Arch. Pompei Oss. Vesuviano (eds.), Archeologie und Seismologie -La Regione Vesuviana dal 62 al 79 D.C. Problemi Archeologici e Sismologici. Biering and Brinkmann, Munich, pp. 131–135.
- Marturano, A., Aiello, G., Barra, D., Fedele, L., Grifa, C., Morra, V., Berg, R., Varone, A., 2009. Evidence for Holocene uplift at Somma-Vesuvius. *J. Volcanol. Geotherm. Res.* 184, 451–461.
- Mattioli, G.S., Voight, B., et al., 2007. Unique and remarkable dilatometer measurements of pyroclastic flow-generated tsunamis. *Geology* 35, 25–28. doi:10.1130/G22931A.1.
- Mele, D., Sulpizio, R., Dellino, P., La Volpe, L., 2010. Stratigraphy and eruptive dynamics of a pulsating Plinian eruption of Somma-Vesuvius: the Pomice di Mercato (8900 years B.P.). *Bull. Volcanol.* doi:10.1007/s00445-010-0407-2.
- Mercalli, G., 1883. Vulcani e fenomeni vulcanici in Italia. Rist. Anast. Forni, 1981.
- Milia, A., Torrente, M.M., Russo, M., Zuppetta, A., 2003a. Tectonics and crustal structure of the Campania continental margin: relationships with volcanism. *Mineral. Petrol.* 79, 33–47.
- Milia, A., Torrente, M.M., Zuppetta, A., 2003b. Debris avalanches off shore of Somma Vesuvius volcano, Italy: implications for volcanic hazard evaluation. *J. Geol. Soc. Lond.* 160, 309–317.
- Milia, A., Raspini, A., Torrente, M.M., 2007. The dark nature of Somma-Vesuvius volcano: evidence from the 3.5 ka BP Avellino eruption. *Quatern. Int.* doi:10.1016/j.quaint.2007.03.001.
- Milia, A., Raspini, A., Torrente, M.M., 2008. The dark nature of Somma-Vesuvius volcano: evidence from the 3.5 ka BP Avellino eruption – Reply. *Quatern. Int.* 192, 110–115.
- Müller, G.W., 1894. Die Ostracoden des Golfes von Neapel und der angrenzenden Meeres-Abschnitte. Fauna und Flora des Golfes von Neapel und der angrenzenden Meeres-Abschnitte, 21 (1–8). Zoologischen Station zu Neapel, pp. 1–404. pl. 40.
- Neef, G., Zhao, J.X., Collyer, K.D., Zhang, F.S., 2003. Late Quaternary uplift and subsidence of the west coast of Tanna, south Vanuatu, southwest Pacific: U-Th ages of raised coral reef in the Median Sedimentary Basin. *Aust. J. Earth Sci.* 50, 39–48.
- Nunziata, C., Natale, M., Luongo, G., Panza, F.G., 2006. Magma reservoir at Mt. Vesuvius: size of the hot, partially molten, crust material detected deeper than 8 km. *Earth Planet. Sci. Lett.* 242, 51–57.
- Okada, Y., 1992. Internal deformation due to shear and tensile faults in a half-space. *Bull. Seism. Soc. Am.* 82, 1018–1040.
- Panza, G.P., Peccerillo, A., Aoudia, A., Farina, B., 2007. Geophysical and petrological modelling of the structure and composition of the crust and upper mantle in complex geodynamic settings: the Tyrrhenian Sea and surroundings. *Earth Sci. Rev.* 80, 1–46.
- Patacca, E., Scandone, P., 2001. Late thrust propagation and sedimentary response in the thrust-belt-foredeep system of the Southern Apennines (Pliocene-Pleistocene). In: Vai, G.B., Martini, I.P. (Eds.), Anatomy of an Orogen: the Apennines and Adjacent Mediterranean Basins. Kluwer Academic Publishers, Great Britain, pp. 401–440.
- Patacca, E., Sartori, R., Scandone, P., 1990. Tyrrhenian basin and apenninic arcs: kinematic relations since late Tortonian times. *Mem. Soc. Geol. Ital.* 45, 425–451.
- Pescatore, T., Senatore, M.R., Capretto, G., Lerro, G., Patricelli, G., 1999. Ricostruzione paleogeografica delle aree circostanti l'antica città di Pompei (Campania, Italia) al tempo dell'eruzione del Vesuvio del 79 d.C. *Boll. Soc. Geol. Ital.* 118, 243–254.
- Pescatore, T., Senatore, M.R., Capretto, G., Lerro, G., 2001. Holocene coast environments near Pompeii before the A.D. 79 eruption of Mount Vesuvius, Italy. *Quatern. Res.* 55, 77–85. doi:10.1006/qres.2000.2186.
- Peypouquet, J.P., Nachite, D., 1984. Les Ostracodes en Méditerranée nord-occidentale. Ecomed, Ass. Franc. Techn. Pétrole, Paris, pp. 151–169.
- Piochi, M., Bruno, P.P., De Astis, G., 2005. Relative roles of rifting tectonics and magma ascent processes: Inferences from geophysical, structural, volcanological and geochemical data for the Neapolitan volcanic region (southern Italy). *Geochem. Geophys. Geosyst.* 6, Q07005. doi:10.1029/2004GC000885.
- Pirazzoli, P.A., 2005. A review of possible eustatic, isostatic, and tectonic contribution in eight Late-Holocene relative sea-level histories from the Mediterranean area. *Quat. Sci. Rev.* 24, 1989–2001.
- Principe, C., Tanguy, J.C., Arrighi, S., Palioti, A., Le Goff, M., Zoppi, U., 2004. Chronology of Vesuvius' activity from A.D. 79 to 1631 based on archeomagnetism of lavas and historical sources. *Bull. Volcanol.* 66, 703–724.
- Pujos, M., 1976. Ecologie des foraminifères benthiques et des thé-camoebiens de la Gironde et au plateau continental Sud-Gascogne: application à la connaissance du Quaternaire terminal de la région Ouest-Gironde. *Mem. Inst. Géol. Bassin Aquitaine* 8, 1–274.
- Reimer, P.G., Baillie, M.G.L., Bard, E., Bayliss, A., Beck, J.W., Bertrand, C.J.H., Blackwell, P.G., Buck, C.E., Burr, G.S., Cutler, K.B., Damon, P.E., Edwards, R.L., Fairbanks, R.G., Friedrich, M., Guilderson, T.P., Hogg, A.G., Hughen, K.A., Kromer, B., McCormac, G., Manning, S., Ramsey, C.B., Reimer, R.W., Remmle, S., Southon, J.R., Stuiver, M., Talamo, S., Taylor, F.W., van der Plicht, J., Weyhenmeyer, C.E., 2004. IntCal04 terrestrial radiocarbon age calibration 0–26 cal kyr BP. *Radiocarbon* 46 (3), 1029–1058.
- Rolandì, G., Maraffi, S., Petrosino, P., Lirer, L., 1993. The Ottaviano eruption of Somma-Vesuvius (8000 years BP): a magmatic alternating fall and flow-forming eruption. *J. Volcanol. Geotherm. Res.* 58, 43–65.
- Rome, D.R., 1964. Ostracodes des environs de Monaco, leur distribution en profondeur, nature des fonds marins explorés. Ostracods as ecological and palaeoecological indicators. Simposio internazionale sotto gli auspici della Fondazione Antonio e Rinaldo Dohrn presso la Stazione Zoologica di Napoli, 10–19 Giugno 1963, 33. Pubblicazioni della Stazione Zoologica di Napoli, pp. 200–212 (Supplemento).
- Sacchi, M., Insinga, D., Milia, A., Molosso, F., Raspini, A., Torrente, M.M., Conforti, A., 2005. Stratigraphic signature of the Vesuvius 79 AD event off the Sarno prodelta system, Naples Bay. In: Trincardi, F., Syvitski, J. (Eds.), Mediterranean Prodelta Systems: Marine Geology, 222–223, pp. 443–469.
- Santacroce, R., Sbrana, A., 2003. Geological map of Vesuvius, S.E.L.C.A ed., Firenze.
- Santacroce, R., Cioni, R., Marianelli, P., Sbrana, A., Sulpizio, R., Zanchetta, G., Donahue, D.J., Joron, J.L., 2008. Age and whole rock-glass compositions of proximal pyroclastics from the major explosive eruptions of Somma-Vesuvius: a review as a tool for distal tephrostratigraphy. *J. Volcanol. Geotherm. Res.* 177, 1–18. doi:10.1016/j.jvolgeores.2008.06.009.
- Sgarrella, F., Barra, D., 1985. Distribuzione dei Foraminiferi bentonici nel Golfo di Salerno (Basso Tirreno, Italia). *Boll. Soc. Nat. Napoli* 93, 1–58.
- Sgarrella, F., Moncharmont Zei, M., 1993. Benthic Foraminifera of the Gulf of Naples (Italy): systematics and autoecology. *Boll. Soc. Paleontologica Ital.* 32 (2), 145–264.

- Sgarrella, F., Barra, D., Impronta, A., 1985. The benthic foraminifers of the Gulf of Policastro (Southern Tyrrhenian Sea, Italy). *Boll. Soc. Nat. Napoli* 92, 67–114.
- Stocchi, P., Spada, G., 2008. Glacio and hydro-isostasy in the Mediterranean Sea: Clark's zones and role of remote ice sheets. *Ann. Geophys.* 50 (6), 741–761.
- Tibaldi, A., Vezzoli, L., 2004. A new type of volcano flank failure: the resurgent caldera sector collapse, Ischia, Italy. *Geophys. Res. Lett.* 31, L14605. doi:10.1029/2004GL020419.
- Tinti, S., Pagnoni, G., Piatanesi, A., 2003. Simulation of tsunamis induced by volcanic activity in the Gulf of Naples (Italy). *Nat. Hazards Earth Syst. Sci.* 3, 311–320.
- Tinti, S., Maramai, A., Graziani, L., 2004. The new catalogue of Italian tsunamis. *Nat. Hazards* 33, 439–465.
- Triantaphyllou, M.V., Tsourou, T., Koukousioura, O., Dermitzakis, M.C., 2005. Foraminiferal and ostracod ecological patterns in coastal environments of SE Andros Island (Middle Aegean Sea, Greece). *Rev. Micropaleontol.* 48 (4), 279–302.
- Uffenorde, H., 1972. Oekologie und jahreszeitliche Verteilung rezenter bentonischer Ostracoden des Limski Kanal bei Rovinj (nördliche Adria). *Göttinger Arb. Geol. Paläontol.* 13, 1–121.
- Vénec-Peyré, M.T., 1984. Ecologie des foraminifères en Méditerranée nord-occidentale. N. Etude de la distribution des foraminifères vivant dans la baie de Banyuls-sur-Mer. Ecologie des microorganismes en Méditerranée occidentale. Ecomed. A.F. T.P. Paris, pp. 60–80.
- Vezzoli, L., 1988. Island of Ischia. *Quaderni di La Ricerca Scientifica*, 114 (10). Consiglio Nazionale delle Ricerche, Roma. 126 pp.
- Vezzoli, L., Principe, C., Malfatti, J., Arrighi, S., Tanguy, J., Le Goff, M., 2009. Modes and times of caldera resurgence: the <10 ka evolution of Ischia Caldera, Italy, from high-precision archaeomagnetic dating. *J. Volcanol. Geotherm. Res.* 186, 305–319.
- Vilardo, G., De Natale, G., Milano, G., Coppa, U., 1996. The seismicity of Mt. Vesuvius. *Tectonophysics* 261, 127–138.
- Vogel, S., Märker, M., 2010. Reconstructing the Roman topography and environmental features of the Sarno River Plain (Italy) before the AD 79 eruption of Somma-Vesuvius. *Geomorphology* 100, 67–77. doi:10.1016/j.geomorph.2009.09.031.
- Walker, G.P.L., 1977. Metodi geologici per la valutazione del rischio vulcanico. Atti del convegno: I vulcani attivi dell'area napoletana. Regione Campania, Napoli, pp. 53–60.
- Westaway, R., 1993. Quaternary uplift of Southern Italy. *J. Geophys. Res.* 98, 741–772.
- Yassini, I., 1979. The littoral system Ostracodes from the bay of Bou-Ismail, Algiers, Algeria. *Rev. Esp. Micropaleontol.* 11 (3), 353–416.
- Zanchetta, G., Sulpizio, R., Di Vito, M.A., 2004. The role of volcanic activity and climate in alluvial fan growth at volcanic areas: an example from southern Campania (Italy). *Sed. Geol.* 168, 249–280.
- Zollo, A., Gasparini, P., Virieux, J., Biella, G., Boschi, E., Capuano, P., de Franco, R., Dell'Aversana, P., De Matteis, R., De Natale, G., Iannaccone, G., Guerra, I., Le Meur, H., Mirabile, L., 1998. An image of Mt. Vesuvius obtained by 2D seismic tomography. *J. Volcanol. Geotherm. Res.* 82, 161–173.
- Zollo, A., Marzocchi, W., Capuano, P., Lomax, A., Iannaccone, G., 2002. Space time behavior of seismic activity at Mt. Vesuvius Volcano, Southern Italy. *Bull. Seismol. Soc. Am.* 92, 625–640.